TECHNICAL REPORT
R-15

APPROXIMATE ANALYTICAL SOLUTIONS FOR HYPERSONIC FLOW OVER SLENDER POWER LAW BODIES

By HAROLD MIRELS

Lewis Research Center
Cleveland, Ohio

CONTENTS

TECHNICAL REPORT R-15

APPROXIMATE ANALYTICAL SOLUTIONS FOR HYPERSONIC FLOW OVER SLENDER POWER LAW BODIES

By Harold Mirels

SUMMARY

Approximate analytical solutions are presented for two-dimensional ($\sigma=0$) and axisymmetric ($\sigma=1$) hypersonic flow over blunt-nosed slender bodies whose shapes follow a power law variation. In particular, the body shape is given by $\bar{r}_b \sim \bar{x}^m$ where $\bar{r}_b$ is the transverse body ordinate, $\bar{x}$ is the streamwise distance from the nose, and m is a constant in the range $2/(\sigma+3)<m<1$. Both zero-order ($M\rightarrow\infty$) solutions and first-order (small but nonvanishing values of $1/(M\delta)^2$) solutions are presented, where M is the free-stream Mach number and δ is a characteristic body or streamline slope. The zero-order shock shape $\overline{R}_0$ is similar to the body shape for these flows. The solutions are found within the framework of hypersonic-slender-body theory.

The limiting case $m=1$ corresponds to a wedge ($\sigma=0$) or cone ($\sigma=1$) flow. The limiting case $m=2/(\sigma+3)$ corresponds to a constant-energy flow ($\bar{r}_b=0$, $\overline{R}_0\sim\bar{x}^{2/(\sigma+3)}$). The latter cases are included so that the present study may be applied to all flows wherein the zero-order shock shape is given by $\overline{R}_0\sim\bar{x}^m$ with m in the range $2/(\sigma+3)\leq m\leq 1$. Flow fields associated with shock shapes having values of m outside this range are also discussed. For all values of m, except $m=1$, certain portions of the flow field violate the hypersonic-slender-body approximations, while other portions are consistent with these approximations. For $m=1$, all portions of the flow field are consistent with the approximations.

The approximate solutions are found as follows. The asymptotic form of the flow in the vicinity of the body surface is used as a guide to write approximate expressions for the dependent variables. These expressions exactly satisfy the continuity and energy equations and contain arbitrary constants which are evaluated so as to satisfy boundary conditions at the shock. The approximate solutions do not satisfy the lateral momentum equation except at the shock and (for the first-order problem) at the body surface.

The results of the approximate solutions are compared with numerical integrations of the equations of motion for various values of m and γ (ratio of specific heats). Good agreement is noted, particularly when m and γ are both near one. The shock is relatively close to the body for the latter cases. Sufficient results are presented to evaluate the accuracy of the approximate method for various values of m and γ.

INTRODUCTION

The steady-state equations of motion for hypersonic flow over slender bodies can be reduced to simpler form by incorporating the "hypersonic-slender-body approximations" (e.g., refs. 1 and 2). The reduced equations are valid provided $\delta^2<<1$ and $1/M\delta\leq 0(1)$, where M is the free-stream Mach number and δ is a characteristic body or streamline slope. Reference 1 has shown that, if the nondimensional streamwise coordinate is considered as a nondimensional time, these reduced equations are identical with the full (exact) equations for a corresponding unsteady flow in one less space variable. Forebody drag on a hypersonic slender body is equivalent to the net energy perturbation (from the undisturbed state) in the corresponding unsteady flow.

References 3 and 4 have treated the constant-energy flow field behind the spherical "blast" wave which is generated when a finite amount of energy is released instantaneously at a point. The analysis assumes a very strong wave and is valid (for a perfect gas) until the decay of shock strength is sufficient to violate the strong shock assumptions. The problem of planar and cylindrical blast waves was treated by a unified analysis in reference 5. In addition, the flow-field modifications associated with more moderate shock strengths were found by a perturbation analysis (refs. 5 and 6). The solution for the cylindrical blast wave was obtained, independently, in reference 7. Reference 8 has pointed out that, within the framework of hypersonic-slender-body theory, the hypersonic flow over a blunt-nosed flat plate (or circular cylinder) may be considered as the steady-state analog of the constant-energy planar or cylindrical blast-wave problems, respectively. The nose drag in the steady problem is equivalent to the finite energy which is instantaneously released in the blast-wave problem. The steady flow is not correct near the nose (where the hypersonic-slender-body approximation $\delta^2 << 1$ is violated) and far downstream of the nose (where the approximation $1/M\delta \leq 0(1)$ is violated as is the strong wave assumptions of blast-wave theory). However, useful results are obtained for the intermediate regions (ref. 8).

The blast-wave problems all exhibit flow similarity. That is, the flow fields at different times are similar, except for a scale factor on both the dependent and independent variables. References 9 and 10 have observed that such similarity exists whenever the shock shape follows a power law variation (with streamwise distance) provided the hypersonic-slender-body equations are considered in the limit as $1/(M\delta)^2 \rightarrow 0$. This led to numerical solutions of the hypersonic flow over slender blunt-nosed bodies. The effect of nonvanishing values of $1/(M\delta)^2$ was also found in reference 10 by a numerical perturbation analysis.

In the present report, approximate analytical solutions are obtained for both the zero-order ($1/(M\delta)^2 \rightarrow 0$) and first-order (small but nonvanishing values of $1/(M\delta)^2$) hypersonic flow over blunt-nosed slender bodies. The zero-order solutions represent generalizations of the approximate analytical solutions of the blast-wave problem which are presented in references 3, 4, and 5. The shock locations and pressure distributions indicated by the approximate solutions are compared with the values which result from a numerical integration of the equations of motion. Finally, some general properties of the hypersonic flow fields associated with power law shock waves are discussed.

ANALYSIS

The equations for hypersonic flow over slender bodies are summarized herein. These are then specialized to obtain the zero-order and first-order equations for hypersonic flow over those slender blunt-nosed bodies whose zero-order shock shape follows a power law variation. Finally, approximate analytical solutions of these equations are obtained.

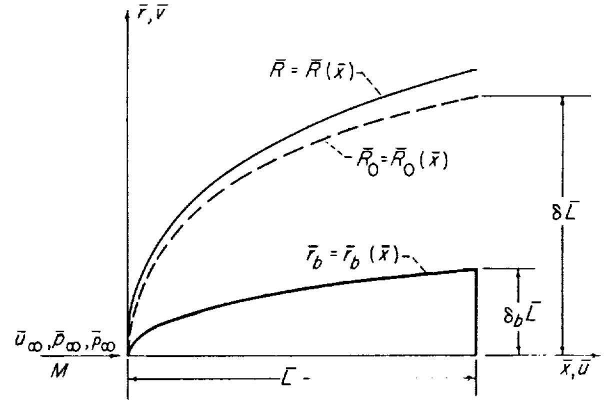

FIGURE 1.—Physical quantities for study of hypersonic flow over blunt-nosed bodies. $\bar{R}_0 = \bar{R}_0(\bar{x})$ is shock shape in the limit as $1/(M\delta)^2 \rightarrow 0$.

HYPERSONIC-SLENDER-BODY THEORY

The equations of motion for hypersonic flow over slender bodies (e.g., ref. 2) are summarized in the present section.

Physical dependent and independent variables are barred herein ($\bar{u}, \bar{v}, \bar{x}, \bar{r}$, etc.). Symbols are defined in appendix A. Figure 1 shows some of these quantities. Let δ represent a characteristic body or streamline slope and $\bar{L}$ represent a characteristic streamwise length. Two-dimensional and axisymmetric flows are considered, with $(\bar{x}, \bar{r})$ and $(\bar{u}, \bar{v})$ being the streamwise and transverse coordinates and velocities, respectively. To obtain the hypersonic-slender-body equations of motion, the following nondimensional quantities are introduced (following ref. 2):

$$\left.\begin{array}{lll} x=\bar{x}/\bar{L} & u=(\bar{u}-\bar{u}_\infty)/\bar{u}_\infty\delta^2 & p=\bar{p}/\gamma M^2\delta^2\bar{p}_\infty \\ r=\bar{r}/\bar{L}\delta & v=\bar{v}/\bar{u}_\infty\delta & \rho=\bar{\rho}/\bar{\rho}_\infty \end{array}\right\} \quad (1)$$

The body shape and shock shape are denoted by $\bar{r}_b = \bar{r}_b(\bar{x})$ and $\bar{R} = \bar{R}(\bar{x})$, respectively, so that

$$r_b = \bar{r}_b/\bar{L}\delta \qquad R = \bar{R}/\bar{L}\delta \quad (2)$$

If these quantities are introduced into the equations of motion and terms of order δ^2 are neglected (compared with one), the hypersonic-slender-

body equations are obtained. These are (ref. 2):
Continuity:

$$\frac{\partial \rho}{\partial x}+\frac{\partial \rho v}{\partial r}+\sigma\frac{\rho v}{r}=0 \tag{3a}$$

r—Momentum:

$$\rho\left(\frac{\partial v}{\partial x}+v\frac{\partial v}{\partial r}\right)+\frac{\partial p}{\partial r}=0 \tag{3b}$$

Energy:

$$\frac{\partial(p/\rho^\gamma)}{\partial x}+v\frac{\partial(p/\rho^\gamma)}{\partial r}=0 \tag{3c}$$

The boundary conditions are:
At body surface:

$$v_b=\frac{dr_b}{dx} \tag{4a}$$

Upstream of shock:

$$u_\infty=v_\infty=0 \tag{4b}$$

$$p_\infty=1/\gamma M^2\delta^2 \tag{4c}$$

$$\rho_\infty=1 \tag{4d}$$

Downstream side of shock:

$$v_s=\frac{2}{\gamma+1}\frac{dR}{dx}\left\{1-\left[1\Big/\left(\frac{dR}{dx}M\delta\right)^2\right]\right\} \tag{4e}$$

$$p_s=\frac{2}{\gamma+1}\left(\frac{dR}{dx}\right)^2\left\{1-\left[\frac{\gamma-1}{2\gamma}\Big/\left(\frac{dR}{dx}M\delta\right)^2\right]\right\} \tag{4f}$$

$$\rho_s=\frac{\gamma+1}{\gamma-1}\Big/\left\{1+\left[\frac{2}{\gamma-1}\Big/\left(\frac{dR}{dx}M\delta\right)^2\right]\right\} \tag{4g}$$

Here $\sigma=0,1$ for two-dimensional and axisymmetric flows, respectively. This system of equations can be solved independent of the x-momentum equation, and therefore the latter is neglected herein. The system of equations is consistent provided $1/M\delta\leq 0(1)$. (Note that the right sides of eqs. (4c), (4e), and (4f) become infinite if $M\delta$ is permitted to go to zero as δ^2 goes to zero.) Thus, the conditions $1/M\delta\leq 0(1)$ and $\delta^2<<1$ must be satisfied for the hypersonic-slender-body equations to be valid.

FLOW FIELDS HAVING ZERO-ORDER SHOCK SHAPES FOLLOWING POWER LAW VARIATION

The equations for hypersonic flow over slender bodies are specialized herein. The resulting equations give the zero-order and first-order hypersonic flow over those blunt-nosed bodies whose zero-order shock shape follows a power law variation. These equations were previously derived in reference 10.

Let $\overline{R}_0(\overline{x})$ denote the shock shape for a given body in the limit as $1/(M\delta)^2\to 0$ (i.e., zero-order solution). References 9 and 10 have shown that when $\overline{R}_0(\overline{x})\sim\overline{x}^m$ the flow fields are similar at each streamwise station (for $1/(M\delta)^2\to 0$). In general, the body shape is similar to the shock shape for such flows, in which case $\overline{r}_b(\overline{x})\sim\overline{x}^m$. Values of m in the range $2/(\sigma+3)<m<1$ correspond to bodies having an infinite positive slope at the nose. The limiting value $m=1$ corresponds to flow over a wedge ($\sigma=0$) or cone ($\sigma=1$), while $m=2/(\sigma+3)$ results in a body shape $\overline{r}_b(\overline{x})=0$. The latter flow may be interpreted as that over a blunt-nosed flat plate ($\sigma=0$) or blunt-nosed circular cylinder ($\sigma=1$). (As in refs. 9 and 10, the $m=2/(\sigma+3)$ case is referred to as the "constant-energy case.") The present report is primarily concerned with values of m in the range $2/(\sigma+3)\leq m\leq 1$.[1] These flows violate the hypersonic-slender-body assumption $\delta^2<<1$ at $\overline{x}\approx 0$ (except for $m=1$) so that the resulting solutions are not expected to be valid in this region.

For the remainder of this report $\overline{L}$ is taken to be the streamwise length of a given body and δ is defined to be

$$\delta=\overline{R}_0(\overline{L})/\overline{L} \tag{5}$$

Then, the nondimensional zero-order shock shape is given by

$$R_0=x^m \tag{6}$$

An alternate characteristic slope based on body thickness at $\overline{x}=\overline{L}$ is

$$\delta_b\equiv\frac{\overline{r}_b(\overline{L})}{\overline{L}}\equiv\delta r_b(1)\equiv\delta\frac{r_b(x)}{R_0(x)} \tag{7}$$

These quantities are indicated in figure 1. For problems where the body shape is initially specified, δ_b is known immediately while δ is found as a consequence of the solution.

New independent variables are now introduced according to the relations

$$\left.\begin{aligned}\xi&=x\\ \eta&=r/R_0=r/x^m\end{aligned}\right\} \tag{8}$$

so that

$$\left.\begin{aligned}\frac{\partial}{\partial x}&=\frac{\partial}{\partial\xi}-\frac{m\eta}{\xi}\frac{\partial}{\partial\eta}\\ \frac{\partial}{\partial r}&=\xi^{-m}\frac{\partial}{\partial\eta}\end{aligned}\right\} \tag{9}$$

[1] Values of m outside this range give rise to flow fields, portions of which are physically realistic and consistent with the assumptions of hypersonic-slender-body theory. These flows are discussed in the section entitled GENERAL CHARACTERISTICS OF FLOW FIELDS ASSOCIATED WITH POWER LAW SHOCKS.

At the zero-order shock location $\eta=1$, and at the body η is also constant and is denoted by η_b. Note also, $\delta_b=\delta\eta_b$. Following references 5, 6, and 10, a small perturbation parameter ϵ is introduced:

$$\left.\begin{aligned}\epsilon&=(\xi^{1-m}/M\delta)^2\\ d\epsilon/dx&=2(1-m)\epsilon/\xi\end{aligned}\right\} \tag{10}$$

The boundary conditions at the shock suggest the following forms for the dependent variables:

$$v=m\,\xi^{m-1}(\varphi_0+\epsilon\varphi_1) \tag{11a}$$

$$p=m^2\xi^{2(m-1)}\,(F_0+\epsilon F_1) \tag{11b}$$

$$\rho=\psi_0+\epsilon\psi_1 \tag{11c}$$

$$R=\xi^m(1+\epsilon a_1) \tag{11d}$$

where φ, F, and ψ are functions of η only and a_1 is a constant which is initially unknown.

An alternate shock shape parameter β can be defined according to the relation

$$\beta\equiv\frac{2}{\sigma+1}\left(\frac{1}{m}-1\right) \tag{12}$$

The range $2/(\sigma+3)\leq m\leq 1$ then corresponds to the range $1\geq\beta\geq 0$. Note, $\beta=1$ corresponds to the constant-energy case.

Substituting these quantities into the equations of motion and collecting terms of order ϵ^0 and ϵ^1 then define the zero-order and first-order approximations, respectively, for the hypersonic flow over a power law body. The choice of the variables is such that the zero-order and first-order equations are functions of η only. These results, which were previously obtained in reference 10, are summarized as follows.

Zero-order approximation.—Equations (3) yield:
Continuity:

$$(\varphi_0-\eta)\psi_0'+\psi_0\varphi_0'+\sigma\frac{\psi_0\varphi_0}{\eta}=0 \tag{13a}$$

η—Momentum:

$$(\varphi_0-\eta)\varphi_0'+\frac{F_0'}{\psi_0}-\left(\frac{\sigma+1}{2}\right)\beta\varphi_0=0 \tag{13b}$$

Energy:

$$(\varphi_0-\eta)\left(\frac{F_0'}{F_0}-\gamma\frac{\psi_0'}{\psi_0}\right)-(\sigma+1)\beta=0 \tag{13c}$$

where primes indicate differentiation with respect to η. The boundary conditions at $\eta=1$ are

$$\left.\begin{aligned}\varphi_0(1)&=F_0(1)=2/(\gamma+1)\\ \psi_0(1)&=(\gamma+1)/(\gamma-1)\end{aligned}\right\} \tag{14}$$

Equations (13) and (14) define the flow field completely. The body location is defined by the tangency condition (eq. (4a)), which becomes (since $r_b=\eta_b R_0$)

$$\varphi_0(\eta_b)=\eta_b \tag{15}$$

Derivatives of the dependent variables, at $\eta=1$, are given in appendix B (for later use).

First-order approximation.—Equations (3) yield, respectively,

$$\varphi_1'+(\varphi_0-\eta)\frac{\psi_1'}{\psi_0}+\left(\frac{\psi_0'}{\psi_0}+\frac{\sigma}{\eta}\right)\varphi_1+\left[(\sigma+1)\beta-(\varphi_0-\eta)\frac{\psi_0'}{\psi_0}\right]\frac{\psi_1}{\psi_0}=0 \tag{16a}$$

$$(\varphi_0-\eta)\varphi_1'+\frac{F_1'}{\psi_0}+\left(\varphi_0'+\frac{\sigma+1}{2}\beta\right)\varphi_1-\frac{F_0'}{\psi_0}\frac{\psi_1}{\psi_0}=0 \tag{16b}$$

$$\gamma\varphi_1'+(\varphi_0-\eta)\frac{F_1'}{F_0}+\left(\frac{F_0'}{F_0}+\frac{\sigma\gamma}{\eta}\right)\varphi_1+\gamma\left(\varphi_0'+\frac{\sigma\varphi_0}{\eta}\right)\frac{F_1}{F_0}=0 \tag{16c}$$

The boundary conditions at $\eta=1$ (see appendix C) are

$$\begin{aligned}\frac{\varphi_1(1)}{1-\varphi_0(1)}&=\left[\frac{-2}{\gamma-1}\left(1+\frac{\sigma+1}{2}\beta\right)^2\right]\\ &\quad-\left\{\frac{\gamma+1}{\gamma-1}\varphi_0'(1)-\frac{2}{\gamma-1}[1+(\sigma+1)\beta]\right\}a_1\\ &\equiv b_{15}-b_{14}a_1\end{aligned} \tag{17a}$$

$$\begin{aligned}\frac{\psi_1(1)}{\psi_0(1)}&=\left[\frac{-2}{\gamma-1}\left(1+\frac{\sigma+1}{2}\beta\right)^2\right]\\ &\quad-\left[\frac{\gamma-1}{\gamma+1}\psi_0'(1)\right]a_1\\ &\equiv b_{25}-b_{24}a_1\end{aligned} \tag{17b}$$

$$\begin{aligned}\frac{F_1(1)}{F_0(1)}&=\left[\frac{-(\gamma-1)}{2\gamma}\left(1+\frac{\sigma+1}{2}\beta\right)^2\right]\\ &\quad-\left\{\frac{\gamma+1}{2}F_0'(1)-2[1+(\sigma+1)\beta]\right\}a_1\\ &\equiv b_{35}-b_{34}a_1\end{aligned} \tag{17c}$$

The tangency condition at the body has already been satisfied (eq. (15)) so that the boundary condition on φ_1 at the body surface is

$$\varphi_1(\eta_b)=0 \tag{18}$$

For a given body, a_1 must be determined such that equations (16) and (17) yield a solution satisfying equation (18). To avoid trial-and-error choices for a_1 in a numerical integration of equations (16) and (17), it is advisable to decompose the dependent variables and boundary conditions into two parts, one independent of a_1 and the other proportional to a_1. That is, each dependent variable is expressed as

$$(\ \ )_1\equiv(\ \ )_{1,1}+(\ \ )_{1,2}a_1 \tag{19}$$

For example, $\varphi_1=\varphi_{1,1}+\varphi_{1,2}a_1$ and so forth. The solution for $(\ \ )_{1,1}$ and $(\ \ )_{1,2}$ can be obtained independent of a_1, and the final solution is given by equation (19) with a_1 found from

$$a_1=-\varphi_{1,1}(\eta_b)/\varphi_{1,2}(\eta_b)$$

Such a procedure was used in references 6 and 10 and is permitted because of the linearity of equations (16) and (17). This procedure was also used herein to get additional numerical integrations of equations (16) and (17). When getting approximate analytical solutions of these equations, it is possible to satisfy equation (18) without resorting to equation (19).

EXPRESSIONS FOR SURFACE PRESSURE, SHOCK SHAPE, AND DRAG

Before continuing with the solution of the zero-order and first-order problems, it is useful to develop expressions for surface pressure, shock shape, and drag for these flows.

Within the framework of hypersonic-slender-body theory, the local pressure coefficient is given by (from eqs. (1))

$$C_p\equiv\frac{\overline{p}-\overline{p}_\infty}{\frac{1}{2}\overline{\rho}_\infty\overline{u}_\infty^2}=2\delta^2\left[p-\frac{1}{\gamma(M\delta)^2}\right] \tag{20}$$

The local surface pressure coefficient for the zero- and first-order problems is then given by either of the following expressions (from eqs. (11b) and (20)):

$$\frac{C_{p,b}}{(d\overline{r}_b/d\overline{x})^2}=\frac{2F_0(\eta_b)}{\eta_b^2}\left\{1+\left[\frac{F_1(\eta_b)}{F_0(\eta_b)}-\frac{1}{\gamma m^2F_0(\eta_b)}\right]\frac{\eta_b^2}{(M\delta_b)^2}\left(\frac{\overline{x}}{\overline{L}}\right)^{2(1-m)}\right\} \tag{21a}$$

or

$$\frac{C_{p,b}}{(d\overline{R}_0/d\overline{x})^2}=2F_0(\eta_b)\left\{1+\left[\frac{F_1(\eta_b)}{F_0(\eta_b)}-\frac{1}{\gamma m^2F_0(\eta_b)}\right]\frac{1}{(M\delta)^2}\left(\frac{\overline{x}}{\overline{L}}\right)^{2(1-m)}\right\} \tag{21b}$$

The equivalence of equations (21a) and (21b) can be seen by noting $\overline{r}_b=\eta_b\overline{R}_0$. Equation (21b) is particularly useful for the $\beta=1$ (constant energy) case since $\overline{r}_b=\eta_b=0$ therein.

The zero-order and first-order shock shapes are given by (from eq. (11d))

$$\frac{\overline{R}(\overline{x})}{\overline{r}_b(\overline{x})}=\frac{1}{\eta_b}\left[1+a_1\frac{\eta_b^2}{(M\delta_b)^2}\left(\frac{\overline{x}}{\overline{L}}\right)^{2(1-m)}\right] \tag{22a}$$

or

$$\frac{\overline{R}(\overline{x})}{\overline{R}_0(\overline{x})}=1+a_1\frac{1}{(M\delta)^2}\left(\frac{\overline{x}}{\overline{L}}\right)^{2(1-m)} \tag{22b}$$

Again, equation (22b) is particularly useful for the $\beta=1$ case, as is discussed later in this section.

Numerical values of the quantities η_b, $F_0(\eta_b)$, $F_1(\eta_b)$, and a_1, which appear in equations (21) and (22), are tabulated in tables I to IV for various values of σ, γ, and β.

The forebody drag can be found by integrating the surface pressures. If $D(\overline{x})$ is the forebody drag up to station $\overline{x}$ and $q\equiv\overline{\rho}_\infty\overline{u}_\infty^2/2$, then the appropriate integral is

$$\frac{D(\overline{x})}{q}=2\pi^\sigma\int_0^{\overline{r}_b(\overline{x})}C_{p,b}(\overline{r}_b)^\sigma\ d\overline{r}_b \tag{23}$$

Noting $\overline{r}_b=\delta_b\overline{L}\xi^m$, substituting equation (21a) into equation (23), and integrating yield for $m>2/(\sigma+3)$

$$\frac{D(\overline{x})}{2\pi^\sigma m^3q\delta_b^2(\overline{L}\delta_b)^{\sigma+1}}=\frac{2F_0(\eta_b)}{\eta_b^2}\left\{\frac{\xi^{m(\sigma+3)-2}}{m(\sigma+3)-2}+\frac{\xi^{m(\sigma+1)}}{m(\sigma+1)}\left[\frac{F_1(\eta_b)}{F_0(\eta_b)}-\frac{1}{\gamma m^2F_0(\eta_b)}\right]\frac{\eta_b^2}{(M\delta_b)^2}\right\} \tag{24}$$

The over-all forebody drag coefficient, referenced to the cross-sectional area of the base, is then

$$C_D\equiv\frac{D(\overline{L})}{2^{1-\sigma}\pi^\sigma q[\overline{r}_b(\overline{L})]^{\sigma+1}}=\frac{2^{\sigma+1}m^3\delta_b^2F_0(\eta_b)}{[m(\sigma+3)-2]\eta_b^2}\left\{1+\frac{m(\sigma+3)-2}{m(\sigma+1)}\left[\frac{F_1(\eta_b)}{F_0(\eta_b)}-\frac{1}{\gamma m^2F_0(\eta_b)}\right]\frac{\eta_b^2}{(M\delta_b)^2}\right\} \tag{25}$$

TABLE I.—APPROXIMATE SOLUTION OF ZERO-ORDER PROBLEM FOR $\sigma=0$ AND COMPARISON WITH RESULTS OF NUMERICAL INTEGRATION OF EQUATIONS OF MOTION

γ	β	Approximate solution				Numerical integration	
		C_0	D_0	η_b	$F_0(\eta_b)$	η_b	$F_0(\eta_b)$
1.15	0	0	1.255	0.930	0.930	0.930	0.930
	1/3	2.93	1.535	.891	.766	.891	.761
	1/2	5.18	1.800	.852	.672	.852	.675
	5/8	7.16	2.13	.801	.598	.803	.611
	3/4	8.52	2.68	.710	.520	.716	.546
	7/8	6.16	3.80	.513	.442	.535	.481
	1	.465	7.67	0	.412	0	.415
1.4	0	0	1.556	0.833	0.833	0.833	0.833
	1/3	.962	1.678	.760	.679	.759	.666
	1/2	1.240	1.779	.695	.584	.695	.581
	5/8	1.296	1.888	.619	.504	.623	.518
	3/4	1.167	2.04	.499	.415	.513	.454
	7/8	.817	2.30	.284	.320	.333	.390
	1	.417	3.50	0	.316	0	.325
1.67	0	0	1.788	0.749	0.749	0.749	0.749
	1/3	.535	1.788	.660	.605	.658	.587
	1/2	.644	1.770	.586	.512	.585	.507
	5/8	.655	1.762	.505	.432	.509	.446
	3/4	.608	1.752	.385	.340	.404	.386
	7/8	.504	1.738	.186	.239	.248	.326
	1	.375	2.49	0	.250	0	.264

TABLE II.—APPROXIMATE SOLUTION OF ZERO-ORDER PROBLEM FOR $\sigma=1$ AND COMPARISON WITH RESULTS OF NUMERICAL INTEGRATIONS OF REFERENCE 10

γ	β	Approximate solution				Numerical integration (ref. 10)	
		C_0	D_0	η_b	$F_0(\eta_b)$	η_b	$F_0(\eta_b)$
1.15	0	−2.53	2.05	0.965	0.947	0.965	0.948
	1/3	+1.636	1.317	.945	.774	.945	.775
	1/2	3.64	1.642	.924	.682	.924	.688
	5/8	5.53	1.981	.897	.608	[a].898	[a].621
	3/4	7.11	2.53	.846	.531	.845	.553
	7/8	5.68	3.62	.724	.453	[a].735	[a].484
	1	.465	7.13	0	.410	0	.411
1.4	0	−1.019	2.11	0.915	0.872	0.915	0.875
	1/3	+.383	1.228	.875	.704	.875	.696
	1/2	.757	1.485	.839	.611	.839	.607
	5/8	.930	1.631	.795	.529	[a].796	[a].538
	3/4	.949	1.798	.719	.438	.725	.467
	7/8	.757	2.03	.561	.337	[a].589	[a].392
	1	.417	2.92	0	.302	0	.311
1.67	0	−0.625	2.16	0.870	0.805	0.870	0.811
	1/3	+.170	1.161	.819	.645	.819	.634
	1/2	.365	1.405	.776	.554	.776	.544
	5/8	.452	1.450	.726	.469	[a].727	[a].474
	3/4	.483	1.457	.644	.370	.652	.403
	7/8	.459	1.436	.480	.257	[a].518	[a].326
	1	.375	1.867	0	.255	0	.241

[a] Numerical integrations for $\beta=5/8$, $7/8$ were not given in ref. 10 and were found as part of the present study.

TABLE III.—APPROXIMATE SOLUTION OF FIRST-ORDER PROBLEM FOR $\sigma=0$ AND COMPARISON WITH RESULTS OF NUMERICAL INTEGRATION

γ	β	Approximate solution					Numerical integration	
		A_1	B_1	C_1	a_1	$F_1(\eta_b)$	a_1	$F_1(\eta_b)$
1.15	0	1.935	0	−13.33	1.000	1.800	1.000	1.800
	⅓	4.47	−.0516	−27.6	1.342	2.78	1.34	2.79
	½	6.91	+.0550	−35.4	1.453	3.03	1.43	3.16
	⅝	9.20	.226	−41.8	1.474	2.95	-----	-----
	¾	11.76	.385	−48.3	1.415	2.57	1.31	2.77
	⅞	15.11	−.0457	−54.3	1.194	1.999	-----	-----
	1	14.82	+6.85	−60.3	.963	.923	1.03	.910
1.4	0	1.857	0	−5.00	1.000	1.548	1.000	1.548
	⅓	3.06	−.1035	−11.28	1.213	2.18	1.21	2.17
	½	4.24	−.1135	−14.15	1.230	2.22	1.21	2.25
	⅝	5.14	−.1110	−16.18	1.192	2.06	-----	-----
	¾	5.98	−.1430	−18.21	1.113	1.764	1.07	1.78
	⅞	6.82	−.386	−20.0	.975	1.397	-----	-----
	1	6.01	2.94	−22.7	.992	.781	.965	.799
1.67	0	1.799	0	−2.99	1.000	1.348	1.000	1.348
	⅓	2.27	−.1000	−6.99	1.140	1.778	1.14	1.77
	½	2.95	−.1237	−8.55	1.130	1.750	1.11	1.78
	⅝	3.43	−.1323	−9.70	1.092	1.599	-----	-------
	¾	3.85	−.1644	−10.83	1.035	1.367	.991	1.39
	⅞	4.22	−.309	−11.90	.956	1.092	-----	-----
	1	3.96	+1.813	−13.22	.940	.700	.930	.707

TABLE IV.—APPROXIMATE SOLUTION OF FIRST-ORDER PROBLEM FOR $\sigma=1$ AND COMPARISON WITH RESULTS OF NUMERICAL INTEGRATION

γ	β	Approximate solution					Numerical integration			
							Present results		Ref. 10	
		A_1	B_1	C_1	a_1	$F_1(\eta_b)$	a_1	$F_1(\eta_b)$	a_1	$F_1(\eta_b)$
1.15	0	1.163	0.00819	−13.16	0.489	1.10	0.489	1.10	0.455	1.10
	⅓	4.03	.229	−34.1	.883	2.55	.885	2.50	.829	2.43
	½	7.33	.696	−48.7	1.083	3.28	1.08	3.37	.982	3.05
	⅝	10.78	1.545	−61.7	1.204	3.52	1.17	3.84	-----	----
	¾	14.53	3.25	−76.4	1.288	3.21	1.18	3.79	1.15	3.53
	⅞	17.00	6.61	−93.2	1.377	2.26	1.10	2.93	-----	----
	1	17.25	3.50	−77.5	1.449	1.064	1.23	1.32	1.07	1.35
1.4	0	1.027	0.00909	−4.83	0.477	0.899	0.476	0.918	0.396	0.92
	⅓	2.74	.1231	−13.39	.802	2.03	.807	1.97	.677	1.93
	½	4.57	.315	−18.83	.931	2.50	.932	2.49	.793	2.38
	⅝	6.21	.676	−23.4	.991	2.59	.976	2.67	-----	----
	¾	7.77	1.391	−28.5	1.027	2.36	.976	2.51	.870	2.36
	⅞	8.73	2.81	−34.2	1.075	1.796	.964	1.95	-----	----
	1	7.67	1.372	−28.3	1.231	.954	.992	1.14	.937	1.07
1.67	0	0.968	0.01858	−2.84	0.467	0.785	0.465	0.783	0.350	0.78
	⅓	1.996	.0966	−8.11	.754	1.692	.762	1.63	.575	1.61
	½	3.19	.225	−11.26	.856	2.03	.863	2.00	.663	1.93
	⅝	4.21	.472	−13.87	.903	2.09	.900	2.11	-----	----
	¾	5.18	.952	−16.69	.933	1.919	.911	1.98	.732	1.76
	⅞	5.83	1.906	−19.85	.974	1.606	.922	1.57	-----	----
	1	5.10	1.056	−17.16	1.118	.823	.969	.931	.826	.90

For $\gamma=1.405$, $\beta=0$, $\sigma=1$, the results of ref. 2 indicate $a_1=0.47$ and $F_1(\eta_b)=0.91$ (found from cone results for $M\delta_b=\infty$, 3.988 therein).

For the constant-energy case, $\beta=1$ or $m=2/(\sigma+3)$, the integration of equation (23) is invalid. However, the drag for the latter case can be expressed in terms of a momentum contour integration. A momentum contour integration indicates that the forebody drag up to any station $\bar{x}$ equals the net energy perturbation of the transverse flow (per unit $\bar{x}$) at that station (e.g., ref. 10). The energy perturbation is taken to be the departure from the free-stream value. Thus, if $\overline{E}$ is the energy perturbation per unit mass at any point,

$$\overline{E}\equiv c_v(\overline{T}-\overline{T}_\infty)+\frac{\bar{v}^2}{2}\equiv\frac{1}{\gamma-1}\left(\frac{\bar{p}}{\bar{\rho}}-\frac{\bar{p}_\infty}{\bar{\rho}_\infty}\right)+\frac{\bar{v}^2}{2} \qquad (26)$$

then

$$D(\bar{x})=2\pi^\sigma\int_{\bar{r}_b(\bar{x})}^{\bar{R}(\bar{x})}\overline{\rho E}\,\bar{r}^\sigma\,d\bar{r} \qquad (27)$$

where

$$\overline{\rho E}=\frac{\gamma m^2}{\gamma-1}(M\delta)^2\bar{p}_\infty\left\{\xi^{2(m-1)}\left(F_0+\frac{\gamma-1}{2}\varphi_0^2\psi_0\right)+\frac{1}{(M\delta)^2}\left[F_1-\frac{\psi_0}{\gamma m^2}+\frac{\gamma-1}{2}\varphi_0^2\psi_0\left(\frac{\psi_1}{\psi_0}+\frac{2\varphi_1}{\varphi_0}\right)\right]\right\} \qquad (28)$$

Noting $\bar{r}=\delta\overline{L}\xi^m\eta$, $d\bar{r}=\delta\overline{L}\xi^m\,d\eta$ and integrating between the limits η_b to $1+\epsilon a_1$ yield

$$\frac{D(\bar{x})}{4\pi^\sigma m^2 q(\delta\overline{L})^{\sigma+1}\delta^2}=\xi^{m(\sigma+3)-2}\int_{\eta_b}^1\left(\frac{F_0}{\gamma-1}+\frac{1}{2}\varphi_0^2\psi_0\right)\eta^\sigma\,d\eta+\frac{\xi^{m(\sigma+1)}}{(\gamma-1)(M\delta)^2}\left\{\frac{4a_1}{\gamma+1}-\frac{1}{\gamma m^2(\sigma+1)}+\int_{\eta_b}^1\left[F_1+\frac{\gamma-1}{2}\varphi_0^2\psi_0\left(\frac{\psi_1}{\psi_0}+\frac{2\varphi_1}{\varphi_0}\right)\right]\eta^\sigma\,d\eta\right\} \qquad (29)$$

wherein use was made of the relation[2] $\int_{\eta_b}^1\psi_0\eta^\sigma\,d\eta=1/(\sigma+1)$. Equation (29) is applicable for all m and is thus more general than equation (24).

Consider the zero-order drag approximation (first term on right side of eq. (29)). It is seen that the dependence on ξ disappears for $m=2/(\sigma+3)$ so that the drag $D(\bar{x})$ and, therefore, the transverse energy jump discontinuously at $\bar{x}=0$ and are constant for $\bar{x}>0$; hence, the origin of the term constant-energy case for this value of m. If the first-order approximation is to be included, equation (29) shows that in order to have a constant-energy flow the value of a_1 must be such as to make the coefficient of $\xi^{m(\sigma+1)}$ identically zero in equation (29). Such constant-energy flows can be used to estimate the shock shape and pressure distribution on blunt-nosed flat plates or circular cylinders (see following sketches). The correspondence between these two flows (sketches (a) and (b)) breaks down at $\bar{x}=0$ because of the finite thickness of the plate or cylinder. However, hypersonic-slender-body theory (which is the starting point of the present analysis) is inapplicable near $\bar{x}=0$ anyhow. These two flows are expected to be in essential agreement in the intermediate regime wherein the values of $\bar{x}$ are neither too small nor too large to invalidate hypersonic-slender-body theory.

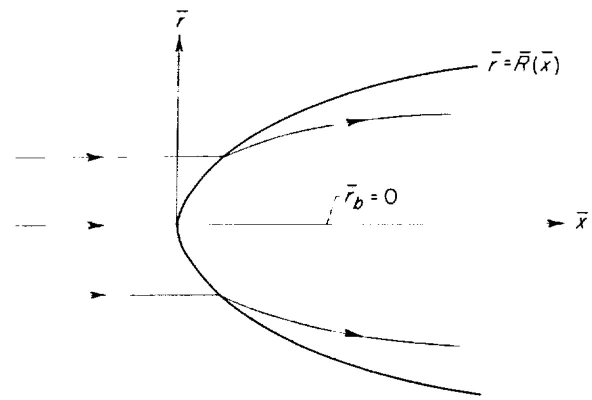

(a) Constant-energy flow. Drag impulse at $\bar{x}=0$.

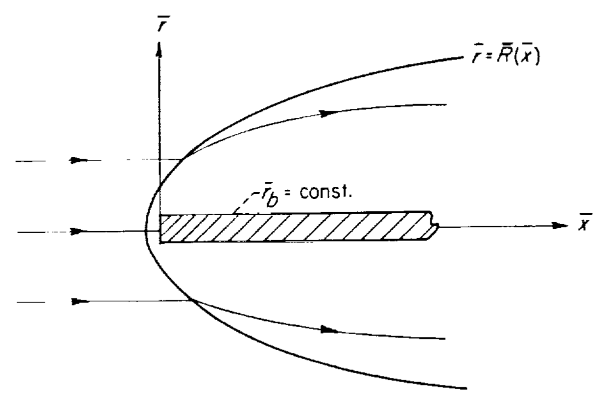

(b) Flow over blunt-nosed plate or circular cylinder. Drag impulse at $\bar{x}=0$.

If the nose drag (i.e., drag impulse at $\bar{x}=0$) is known in a constant-energy problem, it is possible to express the shock shape and pressure distribution as a function of this known nose drag. The

[2] By employing the zero-order stream function (see next section), $\psi_0=\theta_0'/(\sigma+1)\eta^\sigma$, so that $\int_{\eta_b}^1\psi_0\eta^\sigma\,d\eta=[1-\theta_0(\eta_b)]/(\sigma+1)$. For body shapes defined by $\theta_0(\eta_b)=0$, the integral becomes $1/(\sigma+1)$.

procedure is as follows. For a constant-energy flow, equation (29) becomes

$$\frac{D_N}{4\pi^\sigma m^2 q[\overline{R}_0(\overline{x})]^{\sigma+1}[\overline{R}_0(\overline{x})/\overline{x}]^2}=\int_0^1\left(\frac{F_0}{\gamma-1}+\frac{1}{2}\,\varphi_0^2\psi_0\right)\eta^\sigma d\eta\equiv I \quad (30)$$

where D_N is the known nose drag and the substitutions $\overline{L}=\overline{x}$ and $\delta=\overline{R}_0(\overline{x})/\overline{x}$ have been made (since the equation is independent of the choice for $\overline{L}$). Let C_{D_N} be the nose drag coefficient:

$$C_{D_N}\equiv\frac{D_N}{2^{1-\sigma}\pi^\sigma q(\overline{r}_N)^{\sigma+1}} \quad (31)$$

where $\overline{r}_N$ is the half thickness or radius of the flat plate or circular cylinder, respectively. The shock shape can then be expressed as (from eq. (22b))

$$\frac{\overline{R}(\overline{x})}{\overline{r}_N}=\frac{\overline{R}_0(\overline{x})}{\overline{r}_N}\left\{1+a_1\left[\frac{1}{M}\frac{\overline{x}}{\overline{r}_N}\frac{\overline{r}_N}{\overline{R}_0(\overline{x})}\right]^2\right\} \quad (32a)$$

where (from the ratio of eqs. (30) and (31))

$$\frac{\overline{R}_0(\overline{x})}{\overline{r}_N}=\frac{1}{2}\left[\frac{(\sigma+3)^2C_{D_N}}{I}\right]^{\frac{1}{\sigma+3}}\left(\frac{\overline{x}}{\overline{r}_N}\right)^{\frac{2}{\sigma+3}} \quad (32b($$

Equations (32) give the shock shape $\overline{R}(\overline{x})/\overline{r}_N$ as a function of $\overline{x}/\overline{r}_N$ with C_{D_N}, I, and a_1 as parameters. For a given nose configuration, C_{D_N} can be estimated by using methods described in reference 11 and in the references noted therein. Numerical values of I (defined by eq. (30)), obtained from an integration of the zero-order equations, are listed in table V(a) for various γ and σ. These are in good agreement with values reported in reference 5 (table V(b)). The results are expressed as $(\sigma+1)(\gamma^2-1)I$ since this is a slowly varying function of γ and σ. Values of a_1 are listed in tables III and IV for $\sigma=0,1$ and $\gamma=1.15$, 1.4, and 1.67.

The corresponding expression for surface pressure coefficient for the constant-energy case is (from eq. (21b))

$$\frac{C_{p,b}}{(d\overline{R}_0/d\overline{x})^2}=2F_0(0)\left\{1+\left[\frac{F_1(0)}{F_0(0)}-\frac{(\sigma+3)^2}{4\gamma F_0(0)}\right]\left[\frac{1}{M}\frac{\overline{r}_N}{\overline{R}_0(\overline{x})}\frac{\overline{x}}{\overline{r}_N}\right]^2\right\} \quad (33)$$

where $\overline{R}_0(\overline{x})/\overline{r}_N$ is given by equation (32b).

FORMULATION OF ZERO-ORDER PROBLEM IN TERMS OF STREAM FUNCTION

The zero-order and first-order problems could have been formulated in terms of a single dependent variable, the stream function, instead of the three dependent variables p, ρ, and v. Such a formulation is convenient for obtaining asymptotic solutions for the flow in the vicinity of the body. These asymptotic solutions are useful when numerically integrating the equations of motion and when approximate analytical solutions are developed. Hence, the zero-order problem is formulated in terms of a stream function herein, and asymptotic solutions are obtained for η near η_b.

The continuity equation (3a) is satisfied by a stream function $\hat{\psi}$ defined such that

$$\rho=\frac{1}{r^\sigma}\frac{\partial\hat{\psi}}{\partial r}\qquad v=-\frac{\partial\hat{\psi}/\partial x}{\partial\hat{\psi}/\partial r} \quad (34)$$

The energy equation (eq. (3c)) shows that p/ρ^γ is constant along a streamline (except for the dis-

TABLE V.—EVALUATION OF $I\equiv\int_0^1\left(\frac{F_0}{\gamma-1}+\frac{1}{2}\varphi_0^2\psi_0\right)\eta^\sigma d\eta$ AND COMPARISON WITH REFERENCE 5

$(\gamma I\equiv(J_0)_{\text{ref. 5}})$

[Tabulation is in terms of $(\sigma+1)(\gamma^2-1)I$.]

(a) Present results, based on numerical integration of zero-order equations

γ	$(\sigma+1)(\gamma^2-1)I$	
	$\sigma=0$	$\sigma=1$
1.15	1.088	1.098
1.4	1.164	1.203
1.67	1.206	1.278

(b) Values based on Table III of reference 5

γ	$(\sigma+1)(\gamma^2-1)I$		
	$\sigma=0$	$\sigma=1$	$\sigma=2$ (Taylor)
1.2	1.109	1.134	1.134
1.3	1.140	1.170	1.202
1.4	1.163	1.203	1.226
1.667	1.213	1.249	1.293

continuity at the shock). By considering flow downstream of the shock, a function ω (of $\hat{\psi}$) can be defined according to the relation $\omega(\hat{\psi}) \equiv p/\rho^\gamma$ so that

$$p = \omega \rho^\gamma \tag{35}$$

For prescribed shock shapes, the functional dependence of ω on $\hat{\psi}$ can be determined explicitly by considering conditions at the shock. Substitution of the previous equations into the momentum equation reduces the problem to that of determining the single dependent variable $\hat{\psi}$.

In the present section, only the zero-order problem is considered. An appropriate form for $\hat{\psi}_0$ is

$$\hat{\psi}_0 = [1/(\sigma+1)]\xi^{m(\sigma+1)}\theta_0 \tag{36}$$

where $\theta_0 \equiv \theta_0(\eta)$ and $\theta_0(1)=1$. At $\eta=1$, the boundary conditions on p_0 and ρ_0 give

$$\omega_0 = \frac{2}{\gamma+1}\left(\frac{\gamma-1}{\gamma+1}\right)^\gamma m^2 \xi^{2(m-1)} \tag{37a}$$

But, also at $\eta=1$,

$$\hat{\psi}_0 = \frac{\xi^{m(\sigma+1)}}{\sigma+1} \tag{37b}$$

Eliminating ξ between equations (37a) and (37b) and substituting for $\hat{\psi}_0$ according to equation (36) show that

$$\omega_0 = \frac{2m^2}{\gamma+1}\left(\frac{\gamma-1}{\gamma+1}\right)^\gamma [\xi^{m(\sigma+1)}\theta_0]^{-\beta} \tag{38}$$

Therefore, ρ_0, v_0, and p_0 can be expressed as functions of ξ and θ_0 (from eqs. (34), (35), (36), and (38)). Substitution into the momentum equation (eq. (3b)) yields

$$\frac{\theta_0''\theta_0}{(\theta_0')^2} = \frac{\dfrac{\beta}{\gamma} + \dfrac{\sigma}{\eta}\dfrac{\theta_0}{\theta_0'} + \dfrac{(\gamma+1)^{\gamma+1}(\sigma+1)^\gamma}{2\gamma(\gamma-1)^\gamma}\dfrac{\eta^{1+\sigma(\gamma-1)}\theta_0^{1+\beta}}{(\theta_0')^\gamma}\left[\dfrac{\beta}{2} - \left(\sigma + \dfrac{\sigma+1}{2}\beta\right)\dfrac{\theta_0}{\eta\theta_0'}\right]}{1 - \dfrac{(\gamma+1)^{\gamma+1}(\sigma+1)^\gamma}{2\gamma(\gamma-1)^\gamma}\dfrac{\eta^{1+\sigma(\gamma-1)}\theta_0^{1+\beta}}{(\theta_0')^\gamma}\left[\dfrac{(\sigma+1)\theta_0}{\eta\theta_0'}\right]} \tag{39}$$

with the boundary conditions

$$\theta_0(1) = 1$$

$$\theta_0'(1) = \frac{(\sigma+1)(\gamma+1)}{\gamma-1}$$

On the body, $\theta_0(\eta_b)=0$.

The dependent variables of the previous section are related to θ_0 by the relations

$$\varphi_0 = \eta - (\sigma+1)\frac{\theta_0}{\theta_0'} \tag{40a}$$

$$\psi_0 = \frac{1}{\sigma+1}\frac{\theta_0'}{\eta^\sigma} \tag{40b}$$

$$F_0 = \frac{2}{\gamma+1}\frac{1}{\theta_0^\beta}\left(\frac{1}{\sigma+1}\frac{\gamma-1}{\gamma+1}\frac{\theta_0'}{\eta^\sigma}\right)^\gamma \tag{40c}$$

Also,

$$\frac{1-\varphi_0'}{\eta-\varphi_0} = \frac{\theta_0'}{\theta_0} - \frac{\theta_0''}{\theta_0'} \tag{40d}$$

$$\frac{\psi_0'}{\psi_0} = \frac{\theta_0''}{\theta_0'} - \frac{\sigma}{\eta} \tag{40e}$$

$$\frac{F_0'}{F_0} = \gamma\frac{\theta_0''}{\theta_0'} - \beta\frac{\theta_0'}{\theta_0} - \frac{\gamma\sigma}{\eta} \tag{40f}$$

As $\theta_0 \to \theta_0(\eta_b)=0$ (i.e., $\eta \to \eta_b$), the last term in the numerator and denominator of the right side of equation (39) can be neglected (at least for $\beta \leq 1$).[3] Equation (39) can then be written

$$\frac{\theta_0''}{\theta_0'} - \frac{\beta}{\gamma}\frac{\theta_0'}{\theta_0} - \frac{\sigma}{\eta} \approx 0 \tag{41}$$

Integrating gives

$$\theta_0 \approx K_0(\eta^{\sigma+1} - \eta_b^{\sigma+1})^{\gamma/(\gamma-\beta)} \tag{42}$$

where K_0 is a constant. Substitution of equation (42) into equation (39) verifies the neglect of the last terms in the numerator and denominator for η near η_b. An improved asymptotic solution can be obtained by substituting equation (42) into these terms. This gives for $\beta<1$ and $\beta=1$, respectively (recalling $\eta_b=0$ for $\beta=1$),

$$\frac{\theta_0''}{\theta_0'} - \frac{\beta}{\gamma}\frac{\theta_0'}{\theta_0} - \frac{\sigma}{\eta} \approx \left[\frac{(\sigma+1)\beta K_0 \eta_b^{1-\sigma}}{2(\gamma-\beta)F_0(\eta_b)}\right] \times \eta^\sigma(\eta^{\sigma+1} - \eta_b^{\sigma+1})^{\beta/(\gamma-\beta)} \qquad \beta<1$$

$$\approx \left\{\frac{K_0[\gamma(\sigma+3)-2]}{2\gamma^2(\gamma-1)F_0(0)}\right\}\eta^{\frac{\gamma+\sigma}{\gamma-1}} \qquad \beta=1$$

[3] The limit $\beta \leq 1$ is associated with the $\sigma=1$ case (see discussion in section entitled GENERAL CHARACTERISTICS OF FLOW FIELDS ASSOCIATED WITH POWER LAW SHOCKS).

Integrating the expression for $\beta<1$ and then substituting into equations (40a), (40b), and (40c) give, for $\beta<1$,

$$\theta_0\approx K_0[\eta^{\sigma+1}-\eta_b^{\sigma+1}]^{\gamma/(\gamma-\beta)}\left[1+\frac{\beta\eta_b^{1-\sigma}}{2(2\gamma-\beta)F_0(\eta_b)}K_0(\eta^{\sigma+1}-\eta_b^{\sigma+1})^{\gamma/(\gamma-\beta)}\right] \quad (43a)$$

$$\varphi_0-\eta\approx-\frac{\gamma-\beta}{\gamma}\frac{\eta^{\sigma+1}-\eta_b^{\sigma+1}}{\eta^\sigma}\left[1-\frac{\beta\eta_b^{1-\sigma}}{2(2\gamma-\beta)F_0(\eta_b)}\theta_0\right] \quad (43b)$$

$$\psi_0\approx\frac{\gamma K_0}{\gamma-\beta}[\eta^{\sigma+1}-\eta_b^{\sigma+1}]^{\beta/(\gamma-\beta)}\left[1+\frac{\beta\eta_b^{1-\sigma}}{(2\gamma-\beta)F_0(\eta_b)}\theta_0\right] \quad (43c)$$

$$F_0\approx F_0(\eta_b)\left[1+\frac{\beta\eta_b^{1-\sigma}}{2F_0(\eta_b)}\theta_0\right] \quad (43d)$$

Terms of order θ_0^2 are neglected in the brackets of the previous equations. Integrating the expression for $\beta=1$ and then substituting into equations (40a), (40b), and (40c) give, for $\beta=1$,

$$\theta_0\approx K_0\eta^{\frac{(\sigma+1)\gamma}{\gamma-1}}\left[1+\frac{(\sigma+1)K_0\eta}{2\gamma(2\gamma+\sigma-1)F_0(0)}\right]^{\frac{2\gamma+\sigma-1}{\gamma-1}} \quad (43e)$$

$$\varphi_0-\eta\approx-\frac{\gamma-1}{\gamma}\eta\left[1-\frac{1}{2\gamma^2F_0(0)}\eta^{1-\sigma}\theta_0\right] \quad (43f)$$

$$\psi_0\approx\frac{\gamma K_0}{\gamma-1}\eta^{\frac{\sigma+1}{\gamma-1}}\left[1+\frac{3\gamma+\sigma(\gamma+1)-1}{2\gamma^2(2\gamma+\sigma-1)F_0(0)}\eta^{1-\sigma}\theta_0\right] \quad (43g)$$

$$F_0\approx F_0(0)\left[1+\frac{3\gamma+\sigma\gamma-2}{2\gamma(2\gamma+\sigma-1)F_0(0)}\eta^{1-\sigma}\theta_0\right] \quad (43h)$$

Terms of order $(\eta^{1-\sigma}\theta_0)^2$ are neglected. Note, from equations (40c) and (42), that K_0 is related to $F_0(\eta_b)$ by

$$K_0=\left(\frac{\gamma+1}{\gamma-1}\frac{\gamma-\beta}{\gamma}\right)^{\gamma/(\gamma-\beta)}\left[\frac{\gamma+1}{2}F_0(\eta_b)\right]^{1/(\gamma-\beta)}$$

For $\beta=0$ the correction terms vanish in equations (43a) to (43d). A higher order approximation can be obtained, for $\beta=0$, by writing equation (39) as

$$\frac{\theta_0''}{\theta_0'}-\frac{\sigma}{\eta}\approx\left[\frac{-\sigma K_0}{\gamma\eta_b^{2\sigma}F_0(\eta_b)}\right]\eta^\sigma(\eta^{\sigma+1}-\eta_b^{\sigma+1})$$

Integration then gives

$$\theta_0\approx K_0(\eta^{\sigma+1}-\eta_b^{\sigma+1})\left[1-\frac{\sigma}{6\gamma(\sigma+1)K_0\eta_b^{2\sigma}F_0(\eta_b)}K_0^2(\eta^{\sigma+1}-\eta_b^{\sigma+1})^2\right] \quad (43i)$$

$$\varphi_0-\eta\approx-\frac{\eta^{\sigma+1}-\eta_b^{\sigma+1}}{\eta^\sigma}\left[1+\frac{\sigma}{3(\sigma+1)\gamma K_0\eta_b^{2\sigma}F_0(\eta_b)}\theta_0^2\right] \quad (43j)$$

$$\psi_0\approx K_0\left[1-\frac{\sigma}{2(\sigma+1)\gamma K_0\eta_b^{2\sigma}F_0(\eta_b)}\theta_0^2\right] \quad (43k)$$

$$F_0\approx F_0(\eta_b)\left[1-\frac{\sigma}{2(\sigma+1)K_0\eta_b^{2\sigma}F_0(\eta_b)}\theta_0^2\right] \quad (43l)$$

Terms of order θ_0^4 are neglected.

These asymptotic solutions (eqs. (43)) are useful in numerically integrating equation (39) (or eqs. (13)). The boundary conditions at $\eta=1$ permit one to integrate from $\eta=1$ toward $\eta=\eta_b$. However, equation (39) is singular at η_b, and the numerical process breaks down. But, the asymptotic solutions can be used to carry the solution to η_b. For example, if φ_0 is eliminated between equations (40a) and (43b), the resulting equation can be solved for η_b. The result, to the present order, is

$$\eta_b\approx\eta\left\{1-\frac{\gamma(\sigma+1)}{\gamma-\beta}\frac{\theta_0}{\eta\theta_0'}\left[1+\frac{\beta\eta^{1-\sigma}\theta_0}{2(2\gamma-\beta)F_0}\right]\right\}^{1/(\sigma+1)}$$

Similarly, equations (43d) and (43h) give

$$F_0(\eta_b)\approx F_0\left(1-\frac{\beta}{2}\frac{\eta^{1-\sigma}\theta_0}{F_0}\right) \qquad \beta<1$$

$$\approx F_0\left[1-\frac{3\gamma+\sigma\gamma-2}{2\gamma(2\gamma+\sigma-1)}\frac{\eta^{1-\sigma}\theta_0}{F_0}\right] \qquad \beta=1$$

The asymptotic solutions are also useful as guides for setting up approximate analytical solutions of the zero-order equations. This is done in the next section.

APPROXIMATE ANALYTICAL SOLUTION FOR ZERO-ORDER PROBLEM

An approximate analytical solution for the zero-order problem can be obtained in the following manner. Equations (43b), (43f), and (43j) suggest that φ_0 may be approximated by the expression

$$\varphi_0-\eta=-\left(\frac{\gamma-\beta}{\gamma}\right)\frac{1}{\eta^\sigma}(\eta^{\sigma+1}-\eta_b^{\sigma+1})[1-C_0(\eta^{\sigma+1}-\eta_b^{\sigma+1})^{D_0}] \quad (44a)$$

where C_0 and D_0 (as well as η_b) are as yet unknown constants. Differentiation of equation (44a) shows

$$\varphi_0'+\frac{\sigma\varphi_0}{\eta}=(\sigma+1)\left[\frac{\beta}{\gamma}+\frac{\gamma-\beta}{\gamma}C_0(D_0+1)(\eta^{\sigma+1}-\eta_b^{\sigma+1})^{D_0}\right] \tag{44b}$$

$$\varphi_0''+\sigma\left(\frac{\eta\varphi_0'-\varphi_0}{\eta^2}\right)=\frac{\gamma-\beta}{\gamma}(\sigma+1)^2C_0(D_0+1)D_0\eta^{\sigma}(\eta^{\sigma+1}-\eta_b^{\sigma+1})^{D_0-1} \tag{44c}$$

Substituting equations (44a) and (44b) into the continuity equation (eq. (13a)) permits the latter equation to be integrated. The result is

$$\frac{\psi_0}{\psi_0(1)}=\frac{[1-C_0(1-\eta_b^{\sigma+1})^{D_0}]^{1+\frac{\gamma}{(\gamma-\beta)D_0}}}{(1-\eta_b^{\sigma+1})^{\frac{\beta}{\gamma-\beta}}}\times\frac{(\eta^{\sigma+1}-\eta_b^{\sigma+1})^{\frac{\beta}{\gamma-\beta}}}{[1-C_0(\eta^{\sigma+1}-\eta_b^{\sigma+1})^{D_0}]^{1+\frac{\gamma}{(\gamma-\beta)D_0}}} \tag{45}$$

Similarly, integration of the energy equation (eq. (13c)) yields

$$\frac{F_0}{F_0(1)}=\left[\frac{1-C_0(1-\eta_b^{\sigma+1})^{D_0}}{1-C_0(\eta^{\sigma+1}-\eta_b^{\sigma+1})^{D_0}}\right]^{\frac{\gamma(D_0+1)}{D_0}} \tag{46}$$

The constants C_0, D_0, and η_b will be determined so as to satisfy the boundary conditions on $\varphi_0(1)$, $\varphi_0'(1)$, and $\varphi_0''(1)$ as given by equations (14), (B1), and (B4). The resulting solution for φ_0, F_0, and ψ_0 will have the correct values of these functions and their first and second derivatives at $\eta=1$ and will satisfy the auxiliary condition $\varphi_0(\eta_b)=\eta_b$. In addition, the continuity and energy equations are identically satisfied, but the momentum equation is not (except at $\eta=1$).

Note that the expression for θ_0 associated with equation (44a) is (from eq. (40a))

$$\theta_0=exp\left[(\sigma+1)\int_{\eta}^{1}\frac{d\eta}{\varphi_0-\eta}\right] \tag{47}$$

$$=\frac{[1-C_0(1-\eta_b^{\sigma+1})^{D_0}]^{\frac{\gamma}{(\gamma-\beta)D_0}}}{(1-\eta_b^{\sigma+1})^{\frac{\gamma}{\gamma-\beta}}}\times\frac{(\eta^{\sigma+1}-\eta_b^{\sigma+1})^{\frac{\gamma}{\gamma-\beta}}}{[1-C_0(\eta^{\sigma+1}-\eta_b^{\sigma+1})^{D_0}]^{\frac{\gamma}{(\gamma-\beta)D_0}}} \tag{48}$$

Any form for $\varphi_0-\eta$ which permits equation (47) to be integrated in closed form will permit equations (13a) and (13c) to be integrated in closed form. Similarly, equations (45) and (46) could have been deduced from equations (40b), (40c), and (48).

The constants C_0, D_0, and η_b will now be evaluated. The cases $\beta<1$ and $\beta=1$ are treated separately.

Case $\beta<1$.—Define the following known quantities:

$$P_0\equiv\frac{\gamma-1}{\gamma+1}\,\frac{\gamma}{\gamma-\beta} \tag{49a}$$

$$Q_0\equiv\frac{1}{\sigma+1}\,\frac{\gamma}{\gamma-\beta}\left[\varphi_0'(1)+\frac{2\sigma}{\gamma+1}-\frac{(\sigma+1)\beta}{\gamma}\right] \tag{49b}$$

$$S_0\equiv\frac{1}{(\sigma+1)^2}\,\frac{\gamma}{\gamma-\beta}\left[\varphi_0''(1)+\sigma\varphi_0'(1)-\frac{2\sigma}{\gamma+1}\right] \tag{49c}$$

where $\varphi_0'(1)$ and $\varphi_0''(1)$ can be found from equations (B1) and (B4). Equations (44), evaluated at $\eta=1$, become

$$P_0=1-\eta_b^{\sigma+1}-C_0(1-\eta_b^{\sigma+1})^{D_0+1} \tag{50a}$$

$$Q_0=(D_0+1)C_0(1-\eta_b^{\sigma+1})^{D_0} \tag{50b}$$

$$S_0=D_0(D_0+1)C_0(1-\eta_b^{\sigma+1})^{D_0-1} \tag{50c}$$

Solving for D_0, C_0, and η_b yields

$$D_0=\frac{1}{2}\left(\frac{P_0S_0}{Q_0}+Q_0-1\right)+\sqrt{\frac{1}{4}\left(\frac{P_0S_0}{Q_0}+Q_0-1\right)^2+\frac{P_0S_0}{Q_0}} \tag{51a}$$

$$C_0=\frac{Q_0}{D_0+1}\left(\frac{S_0}{D_0Q_0}\right)^{D_0} \tag{51b}$$

$$\eta_b=\left(1-\frac{D_0Q_0}{S_0}\right)^{1/(\sigma+1)} \tag{51c}$$

The pressure distribution is found from

$$F_0(\eta_b)=\frac{2}{\gamma+1}\left(1-\frac{Q_0}{D_0+1}\right)^{\frac{\gamma(D_0+1)}{D_0}} \tag{51d}$$

The constants P_0, Q_0, and S_0 have the following values when $\sigma=0,1$. For $\sigma=0$:

$$P_0=\frac{\gamma-1}{\gamma+1}\,\frac{\gamma}{\gamma-\beta} \tag{52a}$$

$$Q_0=\frac{2\gamma-1}{\gamma+1}\,\frac{\beta}{\gamma-\beta} \tag{52b}$$

$$S_0=\frac{\gamma}{\gamma^2-1}\,\frac{\beta}{\gamma-\beta}\left[(7\gamma-5)-\frac{13\gamma-11}{2}\,\beta\right] \tag{52c}$$

For $\sigma=1$:

$$P_0=\frac{\gamma-1}{\gamma+1}\,\frac{\gamma}{\gamma-\beta} \tag{53a}$$

$$Q_0=\frac{2\gamma-1}{\gamma+1}\,\frac{1}{\gamma-\beta}\left[\beta-\frac{\gamma(\gamma-1)}{(2\gamma-1)(\gamma+1)}\right] \tag{53b}$$

$$S_0=\frac{\gamma}{2(\gamma^2-1)}\,\frac{1}{\gamma-\beta}\left[-(13\gamma-11)\beta^2+\frac{2(9\gamma^2+\gamma-6)}{\gamma+1}\,\beta-\frac{(\gamma-1)(5\gamma^2+10\gamma+1)}{(\gamma+1)^2}\right] \tag{53c}$$

Case $\beta=1$.—For $\beta=1$ it is known that $\eta_b=0$ so that an approximate solution is (from eqs. (50a) and (50b))

$$\eta_b=0 \qquad C_0=1-P_0 \qquad D_0=(Q_0/C_0)-1 \tag{54}$$

This solution does not satisfy the boundary condition on $\varphi_0''(1)$. It gives more accurate results than do equations (49) to (51) evaluated for $\beta=1$.

Equations (54) correspond to the approximate analytical solutions of the zero-order blast-wave problem which are presented in references 3, 4, and 5. Equations (44) to (53) may be viewed as a generalization of the latter for $\beta<1$. An exact closed-form solution for the $\beta=1$ case is presented in reference 10 (for $\sigma=0,1,2$) and in reference 12 (for $\sigma=2$).

Numerical results for $\sigma=0,1$ and various values of β and γ are listed in tables I and II.

APPROXIMATE ANALYTICAL SOLUTION FOR FIRST-ORDER PROBLEM

The quantities $\varphi_1/(\eta-\varphi_0)$, ψ_1/ψ_0, and F_1/F_0 will be considered as the dependent variables (similar to ref. 6). By using equations (40), the first-order equations (eqs. (16)) can then be written, respectively:[4]

Continuity:

$$\left(\frac{\varphi_1}{\eta-\varphi_0}\right)'-\left(\frac{\psi_1}{\psi_0}\right)'+\frac{\theta_0'}{\theta_0}\left(\frac{\varphi_1}{\eta-\varphi_0}+\beta\,\frac{\psi_1}{\psi_0}\right)=0 \tag{55a}$$

Momentum:

$$-(\sigma+1)\left(\frac{\theta_0}{\theta_0'}\right)^2\left(\frac{\varphi_1}{\eta-\varphi_0}\right)'+\frac{F_0\eta^\sigma}{\theta_0'}\left(\frac{F_1}{F_0}\right)'+\frac{\theta_0}{\theta_0'}\left[\frac{\beta(\sigma+1)}{2}-1-2\sigma+2(\sigma+1)\,\frac{\theta_0\theta_0''}{(\theta_0')^2}\right]\left(\frac{\varphi_1}{\eta-\varphi_0}\right)+\frac{F_0'\eta^\sigma}{\theta_0'}\left(\frac{F_1}{F_0}-\frac{\psi_1}{\psi_0}\right)=0 \tag{55b}$$

Energy:

$$\gamma\left(\frac{\varphi_1}{\eta-\varphi_0}\right)'-\left(\frac{F_1}{F_0}\right)'+\left(\frac{\theta_0'}{\theta_0}\right)\left[(\gamma-\beta)\,\frac{\varphi_1}{\eta-\varphi_0}+\beta\,\frac{F_1}{F_0}\right]=0 \tag{55c}$$

First, equations (55a) and (55c) will each be integrated as far as possible.

Equations (55a) and (55c) can be written, respectively:

$$\left(\theta_0^{-\beta}\,\frac{\psi_1}{\psi_0}\right)'=\frac{1}{\theta_0^{1+\beta}}\left(\theta_0\,\frac{\varphi_1}{\eta-\varphi_0}\right)'$$

$$\left(\theta_0^{-\beta}\,\frac{F_1}{F_0}\right)'=\frac{\gamma}{\theta_0^{(\gamma-\beta+\gamma\beta)/\gamma}}\left(\theta_0^{\frac{\gamma-\beta}{\gamma}}\,\frac{\varphi_1}{\eta-\varphi_0}\right)'$$

Integration yields

$$\frac{\psi_1}{\psi_0}=\theta_0^\beta\left[\int\frac{1}{\theta_0^{1+\beta}}\left(\theta_0\,\frac{\varphi_1}{\eta-\varphi_0}\right)'\,\mathrm{d}\eta+\text{const.}\right]$$

$$\frac{F_1}{F_0}=\gamma\theta_0^\beta\left[\int\frac{1}{\theta_0^{(\gamma-\beta+\beta\gamma)/\gamma}}\left(\theta_0^{\frac{\gamma-\beta}{\gamma}}\,\frac{\varphi_1}{\eta-\varphi_0}\right)'\mathrm{d}\eta+\text{const.}\right]$$

Integrating by parts and introducing the constants E_1 and G_1 give the alternate expressions

$$\frac{\psi_1}{\psi_0}=\frac{\varphi_1}{\eta-\varphi_0}+(1+\beta)\theta_0^\beta\int\frac{1}{\theta_0^{1+\beta}}\,\frac{\varphi_1}{\eta-\varphi_0}\,\mathrm{d}\theta_0+E_1\theta_0^\beta \tag{56a}$$

$$\frac{F_1}{F_0}=\frac{\gamma\varphi_1}{\eta-\varphi_0}+(\gamma-\beta+\gamma\beta)\theta_0^\beta\int\frac{1}{\theta_0^{1+\beta}}\,\frac{\varphi_1}{\eta-\varphi_0}\,\mathrm{d}\theta_0+G_1\theta_0^\beta \tag{56b}$$

---

[4] The operation $[\gamma(1+\beta)-\beta]$ (eq. (55a)) $-(1+\beta)$ (eq. (55c)) leads to the special integral

$$\beta\,\frac{\varphi_1}{\eta-\varphi_0}+(\gamma\beta+\gamma-\beta)\,\frac{\psi_1}{\psi_0}-(1+\beta)\,\frac{F_1}{F_0}=(\text{const.})\theta_0^\beta$$

where the constant can be evaluated in terms of the boundary conditions at $\eta=1$.

Substitution of equations (56) into equation (55b) reduces the problem to the single dependent variable $\varphi_1/(\eta-\varphi_0)$. This is essentially what is done in appendix D to obtain the asymptotic form of the first-order solution near $\theta_0 \approx 0$. Since equations (55) are equivalent to a linear third-order equation, three independent asymptotic solutions are obtained. When numerically integrating equations (16) (by the superposition procedure outlined in connection with eq. (19)), the asymptotic solutions are required in order to proceed to η_b from a point near η_b (since the equations are singular at η_b).

An approximate solution of the first-order equations (eqs. (16) to (18)) will be obtained herein by using the asymptotic solutions of appendix D and evaluating the arbitrary constants therein so as to give consistent values for the dependent variables and their first derivatives at $\eta=1$. The asymptotic solutions which do not satisfy $\varphi_1(\eta_b)=0$ are neglected (in order to satisfy eq. (18)). The resulting solution will exactly satisfy the continuity and energy equations but does not satisfy the momentum equation except at $\eta=1$ and $\eta=\eta_b$. The cases $0<\beta<1$, $\beta=0$, and $\beta=1$ are treated separately. In each case the problem is reduced to a form requiring the simultaneous solution of four linear algebraic equations in four unknowns.

Case $0<\beta<1$.—Let $L_{1,1}\equiv-\beta A_1$, $M_{1,1}\equiv\beta(1-\beta)gA_1$, $E_{1,2}\equiv C_1$, and $M_{1,2}\equiv hC_1$ in appendix D. Equations (D4a) plus (D4b) can then be written

$$\frac{\varphi_1}{\eta-\varphi_0}=A_1[-\beta+\beta(1-\beta)g\theta_0]+C_1h\theta_0^{1+\beta}+(2-\beta)B_1\theta_0^2 \tag{57a}$$

$$\frac{\psi_1}{\psi_0}=A_1(1+2\beta g\theta_0)+C_1\theta^{\beta}[1+(2+\beta)h\theta_0]+3B_1\theta_0^2 \tag{57b}$$

$$\frac{F_1}{F_0}=A_1[(\gamma-\beta)+\beta(2\gamma-\beta)g\theta_0]+C_1h(2\gamma+\gamma\beta-\beta)\theta_0^{1+\beta}+(3\gamma-\beta)B_1\theta_0^2 \tag{57c}$$

where

$$g\equiv\frac{-1}{1-\beta}\frac{M_{1,1}}{L_{1,1}}=\frac{-(\gamma-\beta-1)\eta_b^{1-\sigma}}{2(2\gamma-\beta)F_0(\eta_b)}$$

$$h\equiv\frac{M_{1,2}}{E_{1,2}}=\frac{\beta\eta_b^{1-\sigma}}{2(1+\beta)(2\gamma+\beta\gamma-\beta)F_0(\eta_b)}$$

The term involving $B_1\theta_0^2$ was added to equation (57a) so as to permit satisfying an additional boundary condition at $\eta=1$. The corresponding terms in equations (57b) and (57c) were found from equations (56) with $E_1=G_1=0$. Four undetermined constants, A_1, B_1, C_1, and a_1, remain. These are evaluated so as to give consistent values for the dependent variables and their first derivatives at $\eta=1$.

At $\eta=1$, $\theta_0(1)=1$ and equations (57) give (recalling eqs. (17) and (B5))

$$b_{15}-b_{14}a_1=[-\beta+\beta(1-\beta)g]A_1+(2-\beta)B_1+hC_1 \tag{58a}$$

$$b_{25}-b_{24}a_1=(1+2\beta g)A_1+3B_1+[1+(2+\beta)h]C_1 \tag{58b}$$

$$b_{35}-b_{34}a_1=[(\gamma-\beta)+(2\gamma-\beta)\beta g]A_1+(3\gamma-\beta)B_1+(2\gamma+\gamma\beta-\beta)hC_1 \tag{58c}$$

$$b_{45}-b_{44}a_1=\beta(1-\beta)gA_1+2(2-\beta)B_1+(1+\beta)hC_1 \tag{58d}$$

Define the coefficients of A_1, B_1, and C_1 by

$$b_{11}\equiv\beta[(1-\beta)g-1] \qquad b_{12}\equiv2-\beta \qquad b_{13}\equiv h$$

$$b_{21}\equiv1+2\beta g \qquad b_{22}\equiv3 \qquad b_{23}\equiv1+(2+\beta)h$$

$$b_{31}\equiv(\gamma-\beta)+(2\gamma-\beta)\beta g \qquad b_{32}\equiv3\gamma-\beta \qquad b_{33}\equiv(2\gamma+\gamma\beta-\beta)h$$

$$b_{41}\equiv\beta(1-\beta)g \qquad b_{42}\equiv2(2-\beta) \qquad b_{43}\equiv(1+\beta)h$$

Equations (58a) to (58d) can then be written, respectively:

$$\left.\begin{aligned} b_{11}A_1+b_{12}B_1+b_{13}C_1+b_{14}a_1=b_{15}\\ b_{21}A_1+b_{22}B_1+b_{23}C_1+b_{24}a_1=b_{25}\\ b_{31}A_1+b_{32}B_1+b_{33}C_1+b_{34}a_1=b_{35}\\ b_{41}A_1+b_{42}B_1+b_{43}C_1+b_{44}a_1=b_{45}\end{aligned}\right\} \tag{59}$$

which are four simultaneous equations for the four unknowns A_1, B_1, C_1, and a_1. A knowledge of these four quantities, together with equations (57), completely defines the first-order flow field. Numerical results for $\sigma=0,1$ and various values of β and γ are listed in tables III and IV.

Case $\beta=0$.—Let $E_{1,1}\equiv C_1$, $G_{1,2}\equiv A_1$, and $g\equiv\frac{M_{1,1}}{E_{1,1}}\equiv-\frac{M_{1,2}}{G_{1,2}}$ in appendix D. Equations (D5a) and (D5b) become

$$\left.\begin{aligned} \frac{\varphi_1}{\eta-\varphi_0}&=C_1g\theta_0^2-A_1g\theta_0^2+B_1\theta_0^3\\ \frac{\psi_1}{\psi_0}&=C_1\left(1+\frac{3}{2}g\theta_0^2\right)-\frac{3}{2}A_1g\theta_0^2+\frac{4}{3}B_1\theta_0^3\\ \frac{F_1}{F_0}&=\frac{3\gamma}{2}C_1g\theta_0^2+A_1\left(1-\frac{3\gamma}{2}g\theta_0^2\right)+\frac{4\gamma}{3}B_1\theta_0^3\end{aligned}\right\} \tag{60}$$

where

$$g\equiv\frac{-\sigma(\gamma-1)2^{1/\gamma}}{3\gamma(\sigma+1)\eta_b^{2\sigma}[(\gamma+1)F_0(\eta_b)]^{(\gamma+1)/\gamma}}$$

The terms involving $B_1\theta_0^3$ were added so as to permit satisfying an additional boundary condition at $\eta=1$. At $\eta=1$, equations (60) give (using eqs. (17) and (B5))

$$\left.\begin{aligned} b_{15}-b_{14}a_1&=-gA_1+B_1+gC_1\\ b_{25}-b_{24}a_1&=-\frac{3}{2}gA_1+\frac{4}{3}B_1+\left(1+\frac{3}{2}g\right)C_1\\ b_{35}-b_{34}a_1&=\left(1-\frac{3\gamma}{2}g\right)A_1+\frac{4\gamma}{3}B_1+\frac{3\gamma}{2}gC_1\\ b_{45}-b_{44}a_1&=-2gA_1+3B_1+2gC_1\end{aligned}\right\} \tag{61}$$

Define the coefficients of A_1, B_1, and C_1 by

$$\left.\begin{aligned} &b_{11}=-g && b_{12}=1 && b_{13}=g\\ &b_{21}=-\frac{3}{2}g && b_{22}=\frac{4}{3} && b_{23}=1+\frac{3}{2}g\\ &b_{31}=1-\frac{3\gamma}{2}g && b_{32}=\frac{4\gamma}{3} && b_{33}=\frac{3\gamma}{2}g\\ &b_{41}=-2g && b_{42}=3 && b_{43}=2g\end{aligned}\right\} \tag{62}$$

When these quantities are used in equations (59), the unknowns A_1, B_1, C_1, and a_1 can be found, thus defining the first-order flow.

For $\sigma=0$, it can be shown that $A_1=(3\gamma+1)/2\gamma$, $B_1=0$, $C_1=-2/(\gamma-1)$, and $a_1=1$. Also, $F_1(\eta_b)=(3\gamma+1)/[\gamma(\gamma+1)]$. These results are in exact agreement with those from an expansion (in terms of $1/(M\delta)^2$) of the oblique-shock relations for flow over a wedge.

Numerical results are tabulated in tables III and IV.

Case $\beta=1$.—Let $L_{1,1}\equiv-A_1$, $E_{1,2}\equiv C_1$, $g\equiv-M_{1,1}/L_{1,1}$, and $h\equiv M_{1,2}/E_{1,2}$ in appendix D. Equations (D6a) and (D6b) then suggest

$$\left.\begin{aligned} \frac{\varphi_1}{\eta-\varphi_0}&=A_1[-1+(P-1)g\theta_0^P]+C_1h\theta_0^{P+1}+B_1\theta_0^{P+2}\\ \frac{\psi_1}{\psi_0}&=A_1[1+|1-\sigma|(P+1)g\theta_0^P]\\ &\quad+C_1\theta_0\left(1+\frac{P+2}{P}h\theta_0^P\right)+\frac{P+3}{P+1}B_1\theta_0^{P+2}\\ \frac{F_1}{F_0}&=A_1\{(\gamma-1)+[\gamma(P+1)-1]g\theta_0^P\}\\ &\quad+\frac{(\gamma P+2\gamma-1)h}{P}C_1\theta_0^{P+1}+\frac{\gamma P+3\gamma-1}{P+1}B_1\theta_0^{P+2}\end{aligned}\right\} \tag{63}$$

where

$$P\equiv\frac{2\gamma+\sigma-1}{\gamma(\sigma+1)}$$

$$K_0\equiv\left(\frac{\gamma+1}{\gamma}\right)^{\frac{\gamma}{\gamma-1}}\left[\frac{\gamma+1}{2}F_0(0)\right]^{\frac{1}{\gamma-1}}$$

$$g\equiv-\frac{(4\gamma^2-13\gamma-\sigma\gamma+8)K_0^{\frac{(\gamma-1)(\sigma-1)}{\gamma(\sigma+1)}}}{2\gamma^2(\sigma+1)P[\gamma(P+1)-1]F_0(0)}$$

$$h\equiv\frac{(3\gamma+\sigma\gamma-2)PK_0^{\frac{(\gamma-1)(\sigma-1)}{\gamma(\sigma+1)}}}{2\gamma^2(\sigma+1)(P+1)(\gamma P+2\gamma-1)F_0(0)}$$

The terms involving $B_1\theta_0^{P+2}$ were inserted to permit satisfying an additional boundary condition. The solution then proceeds as in the previous cases and results in four simultaneous equations for the four unknowns A_1, B_1, C_1, and a_1. Equations (59) apply with the coefficients of A_1, B_1, and C_1 being given by

$$\left.\begin{aligned}
&b_{11}=(P-1)g-1 && b_{12}=h \\
&b_{21}=1+[1-\sigma](P+1)g && b_{22}=1+[(P+2)h/P] \\
&b_{31}=\gamma-1+[\gamma(P+1)-1]g && b_{32}=[(\gamma P+2\gamma-1)h]/P \\
&b_{41}=(P-1)Pg && b_{42}=(P+1)h \\
&b_{13}=1 \\
&b_{23}=(P+3)/(P+1) \\
&b_{33}=(\gamma P+3\gamma-1)/(P+1) \\
&b_{43}=P+2
\end{aligned}\right\} \quad (64)$$

Equations (59) can be solved for A_1, B_1, C_1, and a_1. Numerical results are given in tables III and IV.

NUMERICAL RESULTS AND DISCUSSION

The zero-order and first-order problems were solved both by numerical integrations of the equations of motion and by the approximate method. The results are tabulated in tables I to IV for $\sigma=0,1$ and various values of β and γ. The results of the numerical integrations of reference 10 are included in tables II and IV. The quantities $F_0(\eta_b)$, $F_1(\eta_b)$, η_b, and a_1 are used in equations (21), (22), (32), and (33) to find pressure distributions and shock shapes for the class of bodies considered in the present report.

With regard to the zero-order problem, tables I and II show that the approximate method is in good agreement with the numerical integrations for β near zero. As β approaches one, the approximate method becomes less accurate. At $\beta=1$, however, the approximate solution is again accurate since the appropriate value $\eta_b=0$ is automatically imposed and there are only two free constants, as opposed to the three free constants in the $\beta\neq1$ cases. In general, the approximate method is accurate when the shock is relatively close to the body (i.e., η_b is near one) so that, for a given β, the approximate solution is most accurate for values of γ near one. The estimates for η_b tend to be more accurate than those for $F_0(\eta_b)$. The variation with η of the dependent variables is plotted in figure 2 for $\sigma=1$, $\gamma=1.4$. Figure 2 is based on the approximate zero-order results. Corresponding figures, from an exact integration of the zero-order equations, are presented in reference 10.

The accuracy of the approximate solution of the first-order equations can be deduced from tables III and IV. Again, the approximate solution tends to be more accurate for β near zero and for γ near one. The accuracy of the first-order approximate solution is less critical than that for the zero-order flow since the former is a perturbation quantity. Thus, if the first-order solution represents a 10-percent correction to the zero-order flow, and, if the approximate first-order solution is 10 percent in error, the latter would represent only a 1-percent error in the over-all flow.

The numerical integrations of the first-order problem, which are reported in reference 10, appear to be in error, particularly with regard to a_1 (see table IV). Note that for $\sigma=1$, $\beta=0$, $\gamma=1.4$ the present approximate method and numerical integrations both give $a_1\approx0.48$, whereas reference 10 gives $a_1\approx0.40$. These can be compared with the value $a_1\approx0.47$ from the cone results of reference 2 (see table IV), indicating better agreement with the present results than with reference 10.

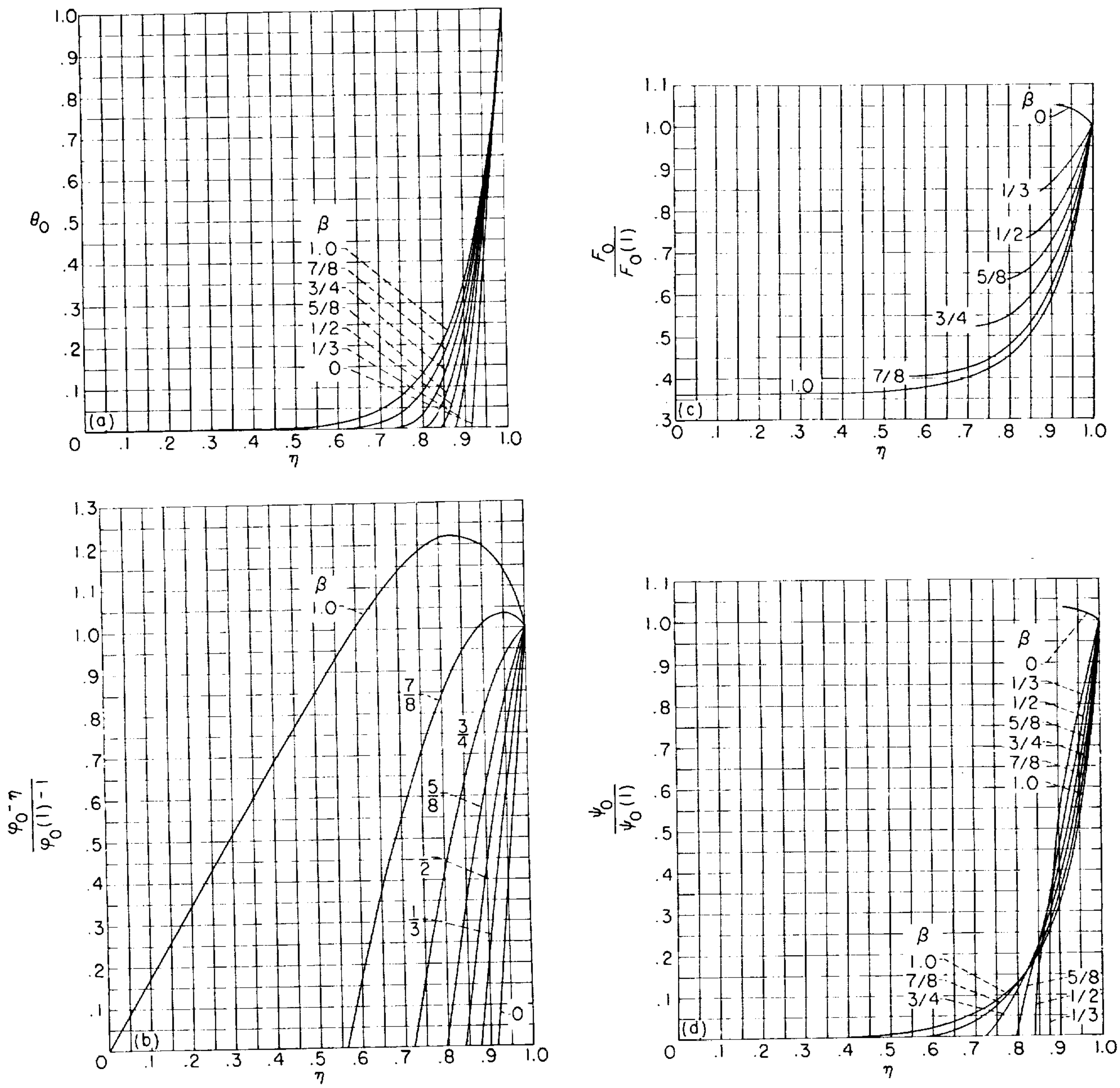

(a) θ_0 plotted against η.

(c) $\frac{F_0}{F_0(1)}$ plotted against η.

(b) $\frac{\varphi_0-\eta}{\varphi_0(1)-1}$ plotted against η.

(d) $\frac{\psi_0}{\psi_0(1)}$ plotted against η.

FIGURE 2.—Results of approximate analytical solution of zero-order problem for $\sigma=1$, $\gamma=1.4$, and various values of β.

GENERAL CHARACTERISTICS OF FLOW FIELDS ASSOCIATED WITH POWER LAW SHOCKS

It was previously shown that, in the limit $1/(M\delta)^2\to 0$, a shock shape of the form $R_0=x^m$ reduces the hypersonic-slender-body equations to a set of ordinary differential equations with $\eta=r/R_0$ as the independent variable. The alternate shock shape parameter $\beta\equiv\left[2\left(\frac{1}{m}-1\right)\right]\Big/(\sigma+1)$ was also introduced. Emphasis was placed on the range $0\leq\beta\leq 1$. In the present section, the general characteristics of the zero-order flow fields associated with different values of β (including $\beta<0$, $\beta>1$) will be discussed.

With $\sigma=0$, equation (39) becomes

$$\left.\begin{aligned}&\frac{\theta_0''\theta_0}{(\theta_0')^2}=\frac{\beta}{\gamma}\,\frac{1+\dfrac{(\gamma+1)^{\gamma+1}}{4(\gamma-1)^{\gamma}}\dfrac{\eta\theta_0^{1+\beta}}{(\theta_0')^{\gamma}}\left(1-\dfrac{\theta_0}{\eta\theta_0'}\right)}{1-\dfrac{(\gamma+1)^{\gamma+1}}{2\gamma(\gamma-1)^{\gamma}}\dfrac{\eta\theta_0^{1+\beta}}{(\theta_0')^{\gamma}}\dfrac{\theta_0}{\eta\theta_0'}}\\ &\theta_0(1)=1 \qquad \theta_0'(1)=(\gamma+1)/(\gamma-1)\end{aligned}\right\}\tag{65}$$

Equation (65) is singular when $\theta_0=0$. The corresponding value of η is denoted by η_b. It can then be shown that for $\theta_0\to 0$, $\eta\to\eta_b$, equation (65) has the following asymptotic forms:

$$\left.\begin{aligned}&\beta<\gamma: &&\theta_0\approx K_0(\eta-\eta_b)^{\frac{\gamma}{\gamma-\beta}} &&\\ &\beta=\gamma: &&\theta_0\approx K_0e^{L_0\eta} &&\eta_b=-\infty\\ &\gamma<\beta<2\gamma: &&\theta_0\approx K_0/(-\eta)^{\frac{\gamma}{\beta-\gamma}} &&\eta_b=-\infty\end{aligned}\right\}\tag{66}$$

where K_0 and L_0 are positive constants. Asymptotic solutions were not found for $\beta\geq 2\gamma$. Also, recall that $\eta_b=0$ for $\beta=1$.

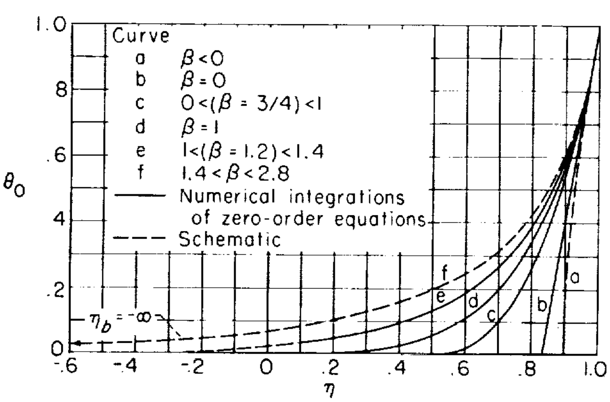

FIGURE 3.—Variation of θ_0 with η for $\sigma=0$, $\gamma=1.4$, and various values of β.

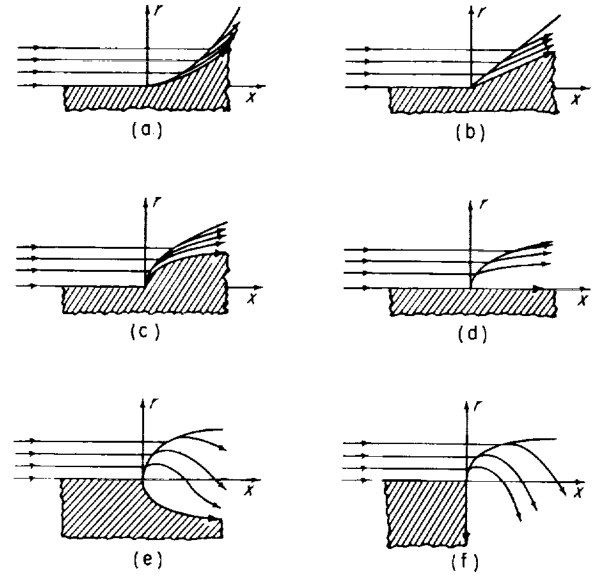

(a) $\beta<0$.
(b) $\beta=0$.
(c) $0<\beta<1$.
(d) $\beta=1$.
(e) $1<\beta<\gamma$.
(f) $\gamma<\beta<2\gamma$.

FIGURE 4.—Schematic representation of flow fields for $\sigma=0$ and various values of β.

The formal solutions of equation (65), for constant γ, can now be represented in the θ_0,η plane for various values of β. This is done in figure 3. The corresponding physical flows are given in figure 4. The value of β defines the shock shape. The corresponding value of η_b defines the body shape (since $r_b=\eta_bR_0$). For η_b positive, the body is in the first quadrant of the x,r plane (figs. 4(a) to (c)), while, for η_b a finite negative number, the body is in the fourth quadrant (fig. 4(e)). The body and shock are similar in shape except for $\eta_b=0,-\infty$. The drag associated with these flows can be found from equation (29). For $\beta>1$ it is seen that the drag is infinite at $x=0$ and thus cannot correspond to a physical situation.

Except for the $\beta=0$ case, each flow field in figure 4 is not everywhere consistent with the original use of the hypersonic-slender-body equations. In particular, conditions at $x=0$ violate the hypersonic-slender-body approximations for all except the $\beta=0$ case. However, in each case, there is a region in the vicinity of the shock (excluding $x\to 0$) for which the flow field is consistent with the approximations. If a streamline in this region is taken to define a body shape (see sketch (c)), then the flow external to this streamline is accurately described, at least initially, by the solutions obtained in the body of the report. Thus, even the $\beta>1$ cases yield flows, portions of which are physically realistic and consistent with the hypersonic-slender-body approximations. The streamlines downstream of the shock are defined, parametrically (with η as parameter), by

$$\frac{x}{x_s}=\left(\frac{1}{\theta_0}\right)^{\frac{1}{m(\sigma+1)}} \qquad \frac{r}{r_s}=\eta\left(\frac{1}{\theta_0}\right)^{\frac{1}{\sigma+1}} \tag{67}$$

where (x_s,r_s) are the coordinates of a streamline at its intersection with the shock. The ratios x/x_s and r/r_s are thus functions only of η (for specified σ, γ, and β). Note that θ_0 and η are not constant along streamlines which do not pass through the origin. The downstream extent to which such solutions are valid has not been resolved.

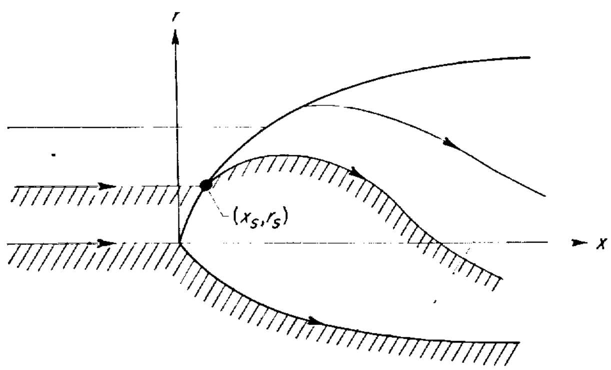

(c) Flow when $\beta>1$.

A similar discussion can be made for the $\sigma=1$ case. Considering equation (39), the asymptotic form for θ_0, as $\theta_0\rightarrow 0$, $\eta\rightarrow\eta_b$, is, for $\beta\leq 1$,

$$\theta_0\approx K_0(\eta^2-\eta_b^2)^{\frac{\gamma}{\gamma-\beta}} \tag{68}$$

where $\eta_b=0$ for $\beta=1$. The asymptotic form when $\beta>1$ has not been determined. Since the flow is axisymmetric, η cannot be negative and the integral curve is confined to the first quadrant of the θ_0,η plane. There is a singularity at $\eta=0$. If a streamline, other than $\theta_0=0$, is taken to define a body, then the external flow corresponds to the flow about an open-nosed body of revolution. The leading-edge angle has a finite nonzero value for such flows.

CONCLUDING REMARKS

An approximate analytical method has been presented for obtaining the zero-order and first-order solutions for hypersonic flow over slender blunt-nosed bodies following a power law variation. Wedge, cone, and constant-energy flows are included as special cases. The solutions are found within the framework of hypersonic-slender-body theory.

The approximate solutions are compared with numerical integrations of the zero- and first-order problems. The agreement is generally good, particularly for β near zero and γ near one. The shock is relatively close to the body for the latter cases. Sufficient numerical results have been tabulated to permit estimates of the accuracy of the approximate method for various combinations of β and γ.

The general characteristics of flow fields associated with power law shocks have also been discussed. It is pointed out that values of the shock shape parameter β outside the range $0\leq\beta\leq 1$ also give rise to flow fields, portions of which are physically realistic and consistent with the hypersonic-slender-body approximations.

The accuracy of the approximate solutions could be improved by following more complex procedures. For example, the flow near the shock can be expanded in a Taylor's series about $\eta=1$, and the flow in the vicinity of the body can be expressed in terms of the asymptotic solutions, each multiplied by an arbitrary constant. These constants can then be evaluated by matching the Taylor's series and the asymptotic expressions at some point between the shock and body. The Taylor's series then represents the flow between the match point and the shock, while the asymptotic expressions represent the flow between the body and the match point.

Lewis Research Center
National Aeronautics and Space Administration
Cleveland, Ohio, *November 17, 1958*

APPENDIX A

SYMBOLS

A_1, B_1, C_1	constants (eqs. (57), et seq.)
a_1	constant (eqs. (11))
b_{ij}	constants (eqs. (17), (B5), (58), et seq.)
C_D	drag coefficient (eq. (25))
C_p	pressure coefficient (eq. (20))
C_0, D_0	constants (eqs. (44))
c_v	specific heat at constant volume
$D(\bar{x})$	forebody drag
$F_0(\eta), F_1(\eta)$	pressure similarity variable (eqs. (11))
I	integral (eq. (30))
K_0	constant (eq. (42))
$\bar{L}$	streamwise length of body
M	free-stream Mach number
m	shock shape power law exponent (eq. (6))
P_0, Q_0, S_0	constants (eqs. (49))
$\bar{p}$	pressure
q	dynamic pressure, $\bar{\rho}_\infty \bar{u}_\infty^2/2$
$\bar{R}(\bar{x})$	lateral displacement of shock
$\bar{R}_0(\bar{x})$	lateral displacement of shock in limit as $1/(M\delta)^2 \rightarrow 0$
$\bar{r}_b(\bar{x})$	body shape
T	temperature
$\bar{u},\bar{v}$	velocities in $(\bar{x},\bar{r})$ direction, respectively
$\bar{x},\bar{r}$	streamwise and lateral coordinates, respectively
β	alternate shock shape parameter, $\left[2\left(\frac{1}{m}-1\right)\right]\Big/(\sigma+1)$
γ	ratio of specific heats
δ	characteristic slope, equals $\bar{R}_0(\bar{L})/\bar{L}$ for flows with power law shocks
δ_b	characteristic body slope, $\bar{r}_b(\bar{L})/\bar{L}$
ϵ	perturbation parameter, $(\xi^{1-m}/M\delta)^2$
η	lateral coordinate similarity variable, r/R_0 (eqs. (8))
$\theta_0(\eta)$	zero-order stream function similarity variable (eq. (36))
ξ	x (eqs. (8))
$\bar{\rho}$	density
σ	0,1,2, for planar, cylindrical, and spherical flow, respectively
$\varphi_0(\eta), \varphi_1(\eta)$	lateral velocity similarity variable (eqs. (11))
$\psi_0(\eta), \psi_1(\eta)$	density similarity variable (eqs. (11))
Subscripts:	
b	quantity evaluated at body surface
s	quantity evaluated at shock
0	zero-order solution
1	first-order solution
∞	undisturbed free-stream value
Superscripts:	
$(\bar{\ })$	barred quantities are dimensional
( )	unbarred quantities are nondimensional (eqs. (1))
( )′	primes indicate differentiation with respect to η

APPENDIX B

DERIVATIVES OF DEPENDENT VARIABLES AT $\eta=1$

The approximate analytic solutions require a knowledge of derivatives of the dependent variables at $\eta=1$. These are summarized as follows.

From equations (13) and (14) it can be shown that

$$\varphi_0'(1)=\frac{1}{(\gamma+1)^2}\,[3(\gamma+1)(\sigma+1)\beta-4\sigma\gamma] \quad \text{(B1)}$$

$$F_0'(1)=\frac{2}{(\gamma-1)(\gamma+1)^2}\,[(2\gamma-1)(\gamma+1)(\sigma+1)\beta-2\sigma\gamma(\gamma-1)] \quad \text{(B2)}$$

$$\psi_0'(1)=\frac{1}{(\gamma-1)^2}\,[3(\gamma+1)(\sigma+1)\beta-2\sigma(\gamma-1)] \quad \text{(B3)}$$

$$\varphi_0''(1)=\frac{2}{\gamma-1}\left\{-\frac{3(\gamma+1)}{\gamma-1}\left(\frac{\sigma+1}{2}\right)^2\beta^2+\left(\frac{3\gamma}{\gamma+1}+\sigma\right)(\sigma+1)\beta-\frac{2\sigma\gamma}{\gamma+1}\right.$$
$$\left.+\left[(5-2\gamma)\left(\frac{\sigma+1}{2}\right)\beta+\frac{\sigma\gamma(\gamma-1)}{\gamma+1}+\frac{\gamma-1}{2}\right]F_0'(1)-\left[(2-\gamma)\left(\frac{\sigma+1}{2}\right)\beta+\frac{\sigma(\gamma-1)^2}{\gamma+1}+\frac{\gamma+1}{2}\right]\varphi_0'(1)\right\} \tag{B4}$$

Similarly, from equations (16) and (17),

$$\frac{1}{\theta_0'(1)}\left(\frac{\varphi_1}{\eta-\varphi_0}\right)'_{\eta=1}=\frac{-2(\gamma-1)}{(\sigma+1)(\gamma+1)^2}\left\{\left[\frac{\gamma+1}{2}F_0'(1)-\frac{\gamma+1}{\gamma-1}\varphi'(1)+\gamma\sigma+\frac{(\gamma+1)(\sigma+1)\beta}{4}+\frac{(\gamma+1)^2}{2(\gamma-1)}\right]\frac{\varphi_1(1)}{1-\varphi_0(1)}\right.$$
$$\left.+\gamma\left[\frac{\gamma+1}{\gamma-1}\varphi_0'(1)+\frac{2\sigma}{\gamma-1}\right]\frac{F_1(1)}{F_0(1)}-\frac{\gamma-1}{2}\left[\frac{\gamma+1}{\gamma-1}\varphi_0'(1)+\frac{(\gamma+1)(\sigma+1)\beta}{(\gamma-1)^2}\right]\frac{\psi_1(1)}{\psi_0(1)}\right\}\equiv b_{45}-b_{44}a_1 \tag{B5}$$

APPENDIX C

BOUNDARY CONDITIONS AT $\eta=1$ FOR FIRST-ORDER PROBLEM

In the first-order problem, the shock is located at $R=\xi^m(1+a_1\epsilon)$ or, equivalently, at $\eta=1+a_1\epsilon$ (see sketch (d)). It is desired to specify boundary conditions at $\eta=1$.

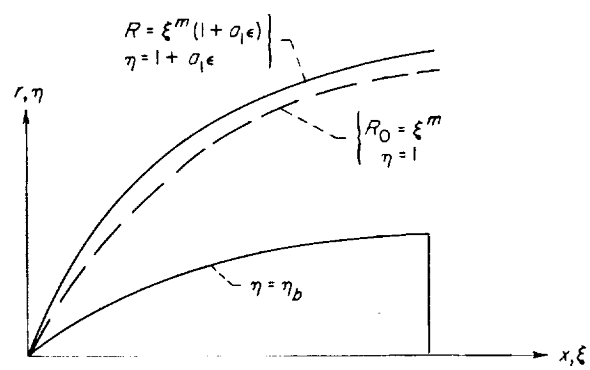

(d) Shock shape.

Let Q be any quantity whose value is known at the downstream side of the shock (designated by subscript s). Then, expanding in a Taylor's series about the shock at constant x yields

$$(Q)_{\eta=1}=(Q)_s+\left(\frac{\partial Q}{\partial r}\right)_s(R_0-R)+\ldots$$
$$=(Q)_s-\left(\frac{\partial Q}{\partial \eta}\right)_s(a_1\epsilon)+\ldots \tag{C1}$$

Consider Q to be the vertical velocity. Equation (C1) becomes

$$v_{\eta=1}=v_s-\left(\frac{\partial v}{\partial \eta}\right)_s a_1\epsilon \tag{C2}$$

But, from equation (4e), $v_s=\frac{2}{\gamma+1}\frac{dR}{dx}\left(1-\frac{\epsilon}{m^2}\right)$, or

$$v_s=\frac{2m}{\gamma+1}\xi^{m-1}\left[1+\epsilon\left(\frac{2-m}{m}a_1-\frac{1}{m^2}\right)\right] \tag{C3}$$

since $dR/dx=m\xi^{m-1}\left[1+\epsilon\left(\frac{2-m}{m}\right)a_1\right]$. Equation (C2) then becomes, by letting $v\equiv m\xi^{m-1}(\varphi_0+\epsilon\varphi_1)$

$$\varphi_0(1)+\epsilon\varphi_1(1)=\frac{2}{\gamma+1}\left[1+\epsilon\left(\frac{2-m}{m}a_1-\frac{1}{m^2}\right)\right]-\varphi_0'(1)a_1\epsilon \tag{C4}$$

so that

$$\varphi_1(1)=\frac{2}{\gamma+1}\left\{-\frac{1}{m^2}+a_1\left[\frac{2-m}{m}-\frac{\gamma+1}{2}\varphi_0'(1)\right]\right\} \tag{C5}$$

Expressions for $F_1(1)$ and $\psi_1(1)$ are found similarly. The results are given in equations (17).

APPENDIX D

ASYMPTOTIC SOLUTIONS OF FIRST-ORDER EQUATIONS

Asymptotic solutions of the first-order equations, near $\theta_0\approx 0$, are found herein.

From equations (56), the continuity and energy equations show

$$\frac{\psi_1}{\psi_0}=\frac{\varphi_1}{\eta-\varphi_0}+(1+\beta)\theta_0^\beta\int\theta_0^{-(1+\beta)}\frac{\varphi_1}{\eta-\varphi_0}\,d\theta_0+E_1\theta_0^\beta \tag{D1a}$$

$$\frac{F_1}{F_0}=\gamma\frac{\varphi_1}{\eta-\varphi_0}+(\gamma+\gamma\beta-\beta)\theta_0^\beta\int\theta_0^{-(1+\beta)}\frac{\varphi_1}{\eta-\varphi_0}\,d\theta_0+G_1\theta_0^\beta \tag{D1b}$$

Consider solutions of the form

$$\frac{\varphi_1}{\eta-\varphi_0}=\theta_0^N(L_1+M_1\theta_0^P+\ldots) \tag{D2a}$$

For $N\neq\beta$, $N+P\neq\beta$, the corresponding values of ψ_1 and F_1 are

$$\frac{\psi_1}{\psi_0}=\theta_0^N\left(\frac{N+1}{N-\beta}L_1+\frac{N+P+1}{N+P-\beta}M_1\theta_0^P+\ldots\right)+E_1\theta_0^\beta \tag{D2b}$$

$$\frac{F_1}{F_0}=\theta_0^N\left[\frac{\gamma N+\gamma-\beta}{N-\beta}L_1+\frac{\gamma(N+P)+\gamma-\beta}{N+P-\beta}M_1\theta_0^P+\ldots\right]+G_1\theta_0^\beta \tag{D2c}$$

The appropriate values of N and P can be found by substituting equations (D2) into the momentum equation (eq. (55b)) and considering $\theta_0\approx 0$. This will be done for $0<\beta<1$, $\beta=0$, and $\beta=1$, respectively.

CASE $0<\beta<1$

In the vicinity of $\theta_0\approx 0$, the momentum equation becomes

$$F_0\eta^\sigma\frac{d(F_1/F_0)}{d\theta_0}+\frac{\beta\eta}{2}\left(\frac{F_1}{F_0}-\frac{\psi_1}{\psi_0}\right)+0\left(\frac{\theta_0}{\theta_0'}\frac{\varphi_1}{\eta-\varphi_0}\right)=0 \tag{D3}$$

Substitution of equations (D2) into (D3) yields the following three independent solutions:

For $N=0$, $P=1$, $E_{1,1}=G_{1,1}=0$:

$$\left.\begin{aligned}
&\frac{\varphi_{1,1}}{\eta-\varphi_0}=L_{1,1}+M_{1,1}\theta_0+\ldots\\
&\frac{\psi_{1,1}}{\psi_0}=-\frac{L_{1,1}}{\beta}+\frac{2M_{1,1}}{1-\beta}\theta_0+\ldots\\
&\frac{F_{1,1}}{F_0}=-\frac{\gamma-\beta}{\beta}L_{1,1}+\frac{2\gamma-\beta}{1-\beta}M_{1,1}\theta_0+\ldots\\
&\frac{M_{1,1}}{L_{1,1}}\equiv\frac{(\gamma-\beta-1)(1-\beta)\eta_b^{1-\sigma}}{2(2\gamma-\beta)F_0(\eta_b)}
\end{aligned}\right\} \tag{D4a}$$

For $N=\beta$, $P=1$, $G_{1,2}=0$:

$$\left.\begin{aligned}
&\frac{\varphi_{1,2}}{\eta-\varphi_0}=\theta_0^\beta(0+M_{1,2}\theta_0+\ldots)\\
&\frac{\psi_{1,2}}{\psi_0}=\theta_0^\beta[E_{1,2}+(2+\beta)M_{1,2}\theta_0+\ldots]\\
&\frac{F_{1,2}}{F_0}=\theta_0^\beta[0+(2\gamma+\gamma\beta-\beta)M_{1,2}\theta_0+\ldots]\\
&\frac{M_{1,2}}{E_{1,2}}\equiv\frac{\beta\eta_b^{1-\sigma}}{2(1+\beta)(2\gamma+\beta\gamma-\beta)F_0(\eta_b)}
\end{aligned}\right\} \tag{D4b}$$

For $N=-(\gamma-\beta)/\gamma$, $P=1$, $E_{1,3}=G_{1,3}=0$:

$$\left.\begin{aligned}
&\frac{\varphi_{1,3}}{\eta-\varphi_0}=\theta_0^{-\frac{\gamma-\beta}{\gamma}}(L_{1,3}+M_{1,3}\theta_0+\ldots)\\
&\frac{\psi_{1,3}}{\psi_0}=\theta_0^{-\frac{\gamma-\beta}{\gamma}}\left[\frac{-\beta L_{1,3}}{\gamma+\gamma\beta-\beta}+\frac{\gamma+\beta}{\beta(1-\gamma)}M_{1,3}\theta_0+\ldots\right]\\
&\frac{F_{1,3}}{F_0}=\theta_0^{-\frac{\gamma-\beta}{\gamma}}\left[0+\frac{\gamma^2M_{1,3}}{\beta(1-\gamma)}\theta_0+\ldots\right]\\
&\frac{M_{1,3}}{L_{1,3}}\equiv\frac{(\gamma-1)\beta^2\eta_b^{1-\sigma}}{2\gamma(\gamma+\gamma\beta-\beta)F_0(\eta_b)}
\end{aligned}\right\} \tag{D4c}$$

For solutions satisfying $\varphi_1(\eta_b)=0$ it is necessary to omit equations (D4c).

CASE $\beta=0$

The momentum equation can be written

$$-(\sigma+1)\,\frac{\theta_0^2}{\theta_0'}\,\frac{\mathrm{d}[\varphi_1/(\eta-\varphi_0)]}{\mathrm{d}\theta_0}+F_0\eta^\sigma\,\frac{\mathrm{d}(F_1/F_0)}{\mathrm{d}\theta_0}$$
$$-\frac{\theta_0}{\theta_0'}\,(1+2\sigma)\left(\frac{\varphi_1}{\eta-\varphi_0}\right)-\frac{\sigma\theta_0}{\theta_0'}\left(\frac{F_1}{F_0}-\frac{\psi_1}{\psi_0}\right)\approx 0$$

where

$$\theta'\approx(\sigma+1)\eta^\sigma K_0\approx(\sigma+1)\eta^\sigma\left(\frac{\gamma+1}{\gamma-1}\right)\left[\frac{\gamma+1}{2}\,F_0(\eta_b)\right]^{1/\gamma}$$

The following three independent solutions result:

For $N=0$, $P=2$, $G_{1,1}=0$:

$$\left.\begin{aligned}
\frac{\varphi_{1,1}}{\eta-\varphi_0}&=0+M_{1,1}\,\theta_0^2+\ \ldots\\
\frac{\psi_{1,1}}{\psi_0}&=E_{1,1}+\frac{3}{2}\,M_{1,1}\,\theta_0^2+\ \ldots\\
\frac{F_{1,1}}{F_0}&=0+\frac{3\gamma}{2}\,M_{1,1}\theta_0^2+\ \ldots\\
\frac{M_{1,1}}{E_{1,1}}&\equiv-\frac{\sigma(\gamma-1)2^{1/\gamma}}{3\gamma(\sigma+1)\eta_b^{2\sigma}[(\gamma+1)F_0(\eta_b)]^{(\gamma+1)/\gamma}}
\end{aligned}\right\}\quad\text{(D5a)}$$

For $N=0$, $P=2$, $E_{1,2}=0$:

$$\left.\begin{aligned}
\frac{\varphi_{1,2}}{\eta-\varphi_0}&=0+M_{1,2}\,\theta_0^2+\ \ldots\\
\frac{\psi_{1,2}}{\psi_0}&=0+\frac{3}{2}\,M_{1,2}\,\theta_0^2+\ \ldots\\
\frac{F_{1,2}}{F_0}&=G_{1,2}+\frac{3\gamma}{2}\,M_{1,2}\,\theta_0^2+\ \ldots\\
\frac{M_{1,2}}{G_{1,2}}&\equiv\frac{\sigma(\gamma-1)2^{1/\gamma}}{3\gamma(\sigma+1)\eta_b^{2\sigma}[(\gamma+1)F_0(\eta_b)]^{(\gamma+1)/\gamma}}\equiv-\frac{M_{1,1}}{E_{1,1}}
\end{aligned}\right\}\quad\text{(D5b)}$$

For $N=-1$, $P=2$, $G_{1,3}=E_{1,3}=0$:

$$\left.\begin{aligned}
\frac{\varphi_{1,3}}{\eta-\varphi_0}&=\theta_0^{-1}(L_{1,3}+M_{1,3}\,\theta_0^2+\ \ldots)\\
\frac{\psi_{1,3}}{\psi_0}&=\theta_0^{-1}(0+2M_{1,3}\,\theta_0^2+\ \ldots)\\
\frac{F_{1,3}}{F_0}&=\theta_0^{-1}(0+2\gamma M_{1,3}\,\theta_0^2+\ \ldots)\\
\frac{M_{1,3}}{L_{1,3}}&\equiv\frac{\sigma(\gamma-1)2^{1/\gamma}}{2\gamma(\sigma+1)\eta_b^{2\sigma}[(\gamma+1)F_0(\eta_b)]^{(\gamma+1)/\gamma}}\equiv-\frac{3}{2}\,\frac{M_{1,1}}{E_{1,1}}
\end{aligned}\right\}\quad\text{(D5c)}$$

When the boundary condition $\varphi_1(\eta_b)=0$ is to be satisfied, equations (D5c) are omitted.

CASE $\beta=1$

For this case, $\eta\approx\eta_b=0,\ \frac{\theta_0}{\theta'\eta}\approx\frac{\gamma-1}{\gamma(\sigma+1)},\ \frac{\theta_0''\theta_0}{(\theta_0')^2}\approx\frac{\gamma\sigma+1}{\gamma(\sigma+1)}$, and $\eta^{1-\sigma}\theta_0\approx K_0\eta^{\frac{2\gamma+\sigma-1}{\gamma-1}}\approx K_0^{\frac{(\gamma-1)(\sigma-1)}{\gamma(\sigma+1)}}\,\theta_0^{\frac{2\gamma+\sigma-1}{\gamma(\sigma+1)}}$.

Recall that

$$K_0=\left(\frac{\gamma+1}{\gamma}\right)^{\frac{\gamma}{\gamma-1}}\left[\frac{\gamma+1}{2}\,F_0(0)\right]^{\frac{\gamma}{\gamma-1}}$$

The momentum equation can be written

$$-\frac{\gamma-1}{\gamma}\,\theta_0\eta^{1-\sigma}\,\frac{\mathrm{d}[\varphi_1/(\eta-\varphi_0)]}{\mathrm{d}\theta_0}+F_0\,\frac{\mathrm{d}(F_1/F_0)}{\mathrm{d}\theta_0}$$
$$+\frac{(\gamma-1)(\sigma\gamma-\gamma+4)}{2\gamma^2(\sigma+1)}\,\eta^{1-\sigma}\,\frac{\varphi_1}{\eta-\varphi_0}$$
$$+\frac{3\gamma+\gamma\sigma-2}{2\gamma^2(\sigma+1)}\,\eta^{1-\sigma}\left(\frac{F_1}{F_0}-\frac{\psi_1}{\psi_0}\right)\approx 0$$

The following three independent solutions are obtained:

For $N=0$, $P=(2\gamma+\sigma-1)/[\gamma(\sigma+1)]$:

(1) $\sigma=0{,}2$ (i.e., $P\neq 1$):

$$\frac{\varphi_{1,1}}{\eta-\varphi_0}=L_{1,1}+(P-1)M_{1,1}\theta_0^P+\ldots$$
$$\frac{\psi_{1,1}}{\psi_0}=-L_{1,1}+(P+1)M_{1,1}\theta_0^P+\ldots$$
$$\frac{F_{1,1}}{F_0}=-(\gamma-1)L_{1,1}+[\gamma(P+1)-1]M_{1,1}\theta_0^P+\ldots$$
$$\frac{M_{1,1}}{L_{1,1}}\equiv\frac{(4\gamma^2-13\gamma-\sigma\gamma+8)K_0^{\frac{(\gamma-1)(\sigma-1)}{\gamma(\sigma+1)}}}{2\gamma^2(\sigma+1)P[\gamma(P+1)-1]F_0(0)}$$

(2) $\sigma=1$ (i.e., $P=1$):

$$\frac{\varphi_{1,1}}{\eta-\varphi_0}=L_{1,1}+0+\ \ldots$$
$$\frac{\psi_{1,1}}{\psi_0}=-L_{1,1}+0+\ \ldots$$
$$\frac{F_{1,1}}{F_0}=-(\gamma-1)\ L_{1,1}+G_{1,1}\theta_0+\ \ldots$$
$$\frac{G_{1,1}}{L_{1,1}}\equiv\frac{2\gamma^2-7\gamma+4}{2\gamma^2F_0(0)}$$

These can be put in the unified form, valid for $\sigma=0,1,2$:

$$\left.\begin{aligned}
\frac{\varphi_{1,1}}{\eta-\varphi_0}&=L_{1,1}+(P-1)\,M_{1,1}\theta_0^P+\ldots\\
\frac{\psi_{1,1}}{\psi_0}&=-L_{1,1}+|1-\sigma|\,(P+1)M_{1,1}\theta_0^P+\ldots\\
\frac{F_{1,1}}{F_0}&=-(\gamma-1)L_{1,1}+[\gamma(P+1)\\
&\qquad -1]M_{1,1}\theta_0^P+\ldots\\
\frac{M_{1,1}}{L_{1,1}}&\equiv\frac{(4\gamma^2-13\gamma-\sigma\gamma+8)K_0^{\frac{(\gamma-1)\,(\sigma-1)}{\gamma\,(\sigma+1)}}}{2\gamma^2(\sigma+1)P[\gamma(P+1)-1]F_0(0)}
\end{aligned}\right\}\quad\text{(D6a)}$$

For $N=1$, $P=(2\gamma+\sigma-1)/[\gamma(\sigma+1)]$, $G_{1,2}=0$:

$$\left.\begin{aligned}
\frac{\varphi_{1,2}}{\eta-\varphi_0}&=\theta_0(0+M_{1,2}\theta_0^P+\ldots)\\
\frac{\psi_{1,2}}{\psi_0}&=\theta_0\left(E_{1,2}+\frac{P+2}{P}M_{1,2}\theta_0^P+\ldots\right)\\
\frac{F_{1,2}}{F_0}&=\theta_0\left(0+\frac{\gamma P+2\gamma-1}{P}M_{1,2}\theta_0^P+\ldots\right)\\
\frac{M_{1,2}}{E_{1,2}}&\equiv\frac{(3\gamma+\sigma\gamma-2)P(K_0)^{\frac{(\gamma-1)(\sigma-1)}{\gamma(\sigma+1)}}}{2\gamma^2(\sigma+1)\,(P+1)\,(\gamma P+2\gamma-1)F_0(0)}
\end{aligned}\right\}\quad\text{(D6b)}$$

For $N=-(\gamma-1)/\gamma$, $P=(2\gamma+\sigma-1)/[\gamma(\sigma+1)]$, $E_{1,3}=G_{1,3}=0$:

$$\left.\begin{aligned}
\frac{\varphi_{1,3}}{\eta-\varphi_0}&=\theta_0^{-\frac{\gamma-1}{\gamma}}\,(L_{1,3}+M_{1,3}\theta_0^P+\ldots)\\
\frac{\psi_{1,3}}{\psi_0}&=\theta_0^{-\frac{\gamma-1}{\gamma}}\left(\frac{L_{1,3}}{1-2\gamma}+\frac{\gamma P+1}{\gamma P+1-2\gamma}M_{1,3}\theta_0^P+\ldots\right)\\
\frac{F_{1,3}}{F_0}&=\theta_0^{-\frac{\gamma-1}{\gamma}}\left(0+\frac{\gamma^2P}{\gamma P+1-2\gamma}M_{1,3}\theta_0^P+\ldots\right)\\
\frac{M_{1,3}}{L_{1,3}}&\equiv-\left[\frac{(3\gamma+\sigma\gamma-2)+(2\gamma-1)\,(\gamma-1)\,(\sigma\gamma-\gamma+4)}{2\gamma^2(\sigma+1)\,(2\gamma-1)}+\left(\frac{\gamma-1}{\gamma}\right)^2\right]\frac{(\gamma P+1-2\gamma)K_0^{\frac{(\gamma-1)(\sigma-1)}{\gamma(\sigma+1)}}}{\gamma P(\gamma P+1-\gamma)F_0(0)}
\end{aligned}\right\}\quad\text{(D6c)}$$

When the boundary condition $\varphi_1(\eta_b)=0$ is to be satisfied, equations (D6c) are omitted.

REFERENCES

1. Hayes, Wallace D.: On Hypersonic Similitude. Quart. Jour. Appl. Math., vol. 5, no. 1, Apr. 1947, pp. 105-106.
2. Van Dyke, Milton D.: A Study of Hypersonic Small-Disturbance Theory. NACA Rep. 1194, 1954. (Supersedes NACA TN 3173.)
3. Taylor, G. I.: The Formation of a Blast Wave by a Very Intense Explosion. Pt. I. Theoretical Discussion. Proc. Roy. Soc. (London), ser. A, vol. 201, no. 1065, Mar. 22, 1950, pp. 159-174.
4. Taylor, G. I.: The Formation of a Blast Wave by a Very Intense Explosion. Pt. II. The Atomic Explosion of 1945. Proc. Roy. Soc. (London), ser. A, vol. 201, no. 1065, Mar. 22, 1950, pp. 175-186.
5. Sakurai, Akira: On the Propagation and Structure of a Blast Wave, I. Jour. Phys. Soc. (Japan), vol. 8, no. 5, Sept.-Oct. 1953, pp. 662-669.
6. Sakurai, Akira: On the Propagation and Structure of a Blast Wave, II. Jour. Phys. Soc. (Japan), vol. 9, no. 2, Mar. Apr. 1954, pp. 256-266.
7. Lin, S. C.: Cylindrical Shock Waves Produced by Instantaneous Energy Release. Jour. Appl. Phys., vol. 25, no. 1, Jan. 1954, pp. 54-57.
8. Cheng, H. K., and Pallone, A. J.: Inviscid Leading-Edge Effect in Hypersonic Flow. Jour. Aero. Sci., vol. 23, no. 7, July 1956, pp. 700-702.
9. Lees, Lester, and Kubota, Toshi: Inviscid Hypersonic Flow Over Blunt-Nosed Slender Bodies. Jour. Aero. Sci., vol. 24, no. 3, Mar. 1957, pp. 195-202.
10. Kubota, Toshi: Investigation of Flow Around Simple Bodies in Hypersonic Flow. Memo. 40, Guggenheim Aero. Lab., C.I.T., June 25, 1957. (Contract DA 04-495-ORD-19.)
11. Van Dyke, Milton D.: The Supersonic Blunt Body Problem—Review and Extension. Jour. Aero/Space Sci., vol. 25, no. 8, Aug. 1958, pp. 485-496.
12. Latter, R.: Similarity Solution for a Spherical Shock Wave. Jour. Appl. Phys., vol. 26, no. 8, Aug. 1955, pp. 954-961.

U.S. GOVERNMENT PRINTING OFFICE: 1959